Supporting Information

Metal-Cation-Induced Shifts in Thiolate Redox and Reduced Sulfur Speciation

W. T. Michael Seo, Madeline N. Riffel, Allen G. Oliver, and Emily Y. Tsui*

Department of Chemistry and Biochemistry, University of Notre Dame, Notre Dame, Indiana 46556, United States

Email: *etsui@nd.edu*

Table of Contents

General Considerations. Unless indicated otherwise, reactions were carried out in oven-dried glassware in a MBraun glovebox under an atmosphere of purified nitrogen. Anhydrous CH_3CN was dried using the Grubbs method on a J.C. Meyer solvent system.[1] CD_3CN was dried over CaH_2 and vacuum transferred before use. DMSO-d_6 was distilled three times from molecular sieves. Celite was dried under vacuum at 300 °C for 3 days. ^{1}H, ^{13}C, and ^{19}FNMR spectra were recorded on a Bruker 400 MHz instrument, a Bruker 500 MHz instrument, or a Varian 600 MHz instrument with shifts reported relative to the residual solvent peak (^{1}H, δ 1.94 ppm and ^{13}C, δ 1.32 ppm for CD_3CN), or to the lock signal for ^{19}F spectra. ^{113}Cd NMR were recorded on a Bruker 500 MHz instrument with shifts reported relative to a $Cd(ClO_4)_2$ standard in D_2O (δ 0 ppm). Elemental analysis was performed by Midwest Microlabs, LLC, Indianapolis, IN. Electronic absorption spectra were taken on an Agilent Cary 60 spectrophotometer. Electrospray ionization mass spectroscopy (ESI-MS) was performed at the University of Notre Dame Spectrometry & Proteomics Facility on a Bruker microTOF-Q II instrument. Powder X-ray diffraction (PXRD) data were collected as solid samples or solutions drop-cast on a glass slide using a Bruker AXS D8 Advance diffractometer at a step rate of 0.2° from a 2θ value of 10–80°. Cyclic voltammetry was performed using a Princeton Applied Research VersaSTAT 4 potentiostat. Voltammograms were obtained using a glassy carbon working electrode and platinum wire counter electrode. Potentials were referenced to the ferrocenium/ferrocene (Fc^+/Fc) couple. Unless otherwise indicated, a scan rate of 0.1 V/s was used.

Unless otherwise indicated, all commercial chemicals were used without further purification. *p*-Toluenethiol was purchased from TCI. 4-Chlorobenzenethiol was purchased from Sigma Aldrich. 4-Fluorobenzenethiol was purchased from Oakwood Chemicals. 4-Trifluorobenzenethiol, lithium triflate, sodium triflate, potassium triflate, magnesium triflate, calcium triflate, and scandium triflate were purchased from Ambeed. Sodium bis(trmethylsilyl)amide was purchased from Acros. Tetrabutylammonium hexafluorophosphate ($TBAPF_6$) was recrystallized twice from ethanol and thoroughly dried under high vacuum before use in voltammetry experiments. Cadmium triflate was prepared following literature procedures.[2]

Synthetic Procedures

Representative synthesis of tetraethylammonium benzenethiolate salts [Et_4N][4-R-C_6H_4S] ([1^R], R = Me, Cl, F, CF_3). In the glovebox, a Schlenk flask equipped with stir bar was charged with a solution of sodium bis(trimethylsilyl)amide (0.183 g, 1.00 mmol) in THF (5 mL). A solution of 4-substituted benzenethiol (1.00 mmol, 1 equiv) in THF (5 mL) was added via syringe while stirring. The reaction was concentrated in vacuo and the resulting residue washed with Et_2O (2 × 5 mL). The solid was dissolved in CH_3CN (10 mL), Et_4NCl added (0.166 g, 1.00 mmol, 1 equiv), and the reaction mixture stirred at RT for 1 h. The mixture was filtered through Celite, concentrated in vacuo, and extracted with THF (10 mL). The solution was concentrated in vacuo to yield the desired product as a colorless, crystalline solid.

[Et_4N][1^{Me}]. Yield: 87%. ^{1}H NMR (600 MHz, CD_3CN) δ 7.03 (d, J = 8.0 Hz, 2H), 6.55 (d, J = 8.0 Hz, 2H), 3.16 (q, J = 7.2 Hz, 8H), 2.10 (s, 3H), 1.20 (t, J = 7.2 Hz, 12H).

[Et$_4$N][1^{F}]. Yield: 65%. ^{1}H NMR (600 MHz, CD_3CN) δ 7.32 – 7.17 (m, 2H), 7.01 – 6.80 (m, 2H), 3.17 (q, *J* = 7.3 Hz, 8H), 1.20 (t, 7.3 Hz, 12H). ^{19}F NMR (471 MHz, CD_3CN) δ -135.03 ppm.

[Et$_4$N][1^{Cl}]. Yield: 96%. ^{1}H NMR (600 MHz, CD_3CN) δ 7.10 (d, *J* = 8.5 Hz, 2H), 6.66 (d, *J* = 8.5 Hz, 2H), 3.16 (q, *J* = 7.3 Hz, 8H), 1.20 (t, *J* = 7.3 Hz, 12H).

[Et$_4$N][1^{CF3}]. Yield: 49%. ^{1}H NMR (600 MHz, CD_3CN) δ 7.15 – 6.95 (m, 2H), 6.56 – 6.35 (m, 2H), 3.16 (q, *J* = 7.3 Hz, 6H), 1.20 (t, *J* = 7.3 Hz, 12H). ^{19}F NMR (471 MHz, CD_3CN) δ -64.17 ppm.

Representative synthesis of tetraethylammonium tetrabenzenethiolatozincate salts ([Et$_4$N]$_2$[4^{R}], R = Me, Cl, F, CF$_3$). Syntheses were adapted from literature procedure.[3] Under ambient conditions, a 20 mL scintillation vial equipped with a stir bar was charged with a solution of 4-substituted thiophenol (0.041 mol, 6.9 equiv), tetraethylammonium chloride (2.25 g, 0.014 mol, 2.3 equiv), and zinc nitrate hexahydrate (1.79 g, 0.006 mol, 1 equiv) in 10 mL methanol. Triethylamine (5.8 mL, 0.041 mol, 6.9 equiv) was added dropwise and the mixture was allowed to stir for 5 min. The reaction mixture was then stored at −30°C overnight. The resulting solid was filtered and recrystallized from hot CH_3CN, filtered, washed with Et_2O, and dried in vacuo to give the desired product.

[Et$_4$N]$_2$[4^{Me}]. Yield: 52%. ^{1}H NMR (600 MHz, CD_3CN) δ 7.39 (d, *J* = 7.8 Hz, 8H), 6.65 (d, *J* = 7.7 Hz, 8H), 3.12 (q, *J* = 7.3 Hz, 16H), 2.14 (s, 1H), 1.17 (t, *J* = 7.3 Hz, 24H) ppm. ^{13}C NMR (126 MHz, CD_3CN) δ 133.77, 129.43, 128.47, 118.30, 53.18 – 52.95 (m), 20.83, 7.76 ppm. Anal. Calcd. for $C_{44}H_{68}N_2S_4Zn$: C, 64.55; H, 8.37; N, 3.42. Found: C, 64.83; H, 8.43; N, 3.44.

[Et$_4$N]$_2$[4^{Cl}]. Yield: 84%. ^{1}H NMR (600 MHz, CD_3CN) δ 7.44 (d, *J* = 8.3 Hz, 8H), 6.80 (d, *J* = 8.3 Hz, 8H), 3.15 (q, *J* = 7.3 Hz, 16H), 1.31 – 1.14 (t, *J* = 7.3 Hz, 24H). ^{13}C NMR (126 MHz, CD_3CN) δ 135.19, 127.41, 125.85, 118.30, 62.68 – 41.85 (m), 7.71 ppm. Anal. Calcd. for $C_{40}H_{56}Cl_4N_2S_4Zn$: C, 53.36; H, 6.27; N, 3.11. Found: C, 53.63; H, 6.38; N, 3.17.

[Et$_4$N]$_2$[4^{F}]. Yield: 51%. ^{1}H NMR (500 MHz, CD_3CN) δ 7.44 (d, *J* = 8.7, 8H), 6.59 (t, *J* = 8.7 Hz, 8H), 3.13 (q, *J* = 7.3 Hz, 16H), 1.17 (t, *J* = 7.3 Hz, 24H) ppm. ^{13}C NMR (126 MHz, CD_3CN) δ 160.55, 134.69 (d, *J* = 6.8 Hz), 118.30, 114.18 (d, *J* = 20.6 Hz), 65.38 – 37.73 (m), 7.73 ppm. ^{19}F NMR (471 MHz, CD_3CN) δ -130.14 ppm. Anal. Calcd. for $C_{40}H_{56}F_4N_2S_4Zn$: C, 57.57; H, 6.76; N, 3.36. Found: C, 57.32; H, 6.85; N, 3.91.

[Et$_4$N]$_2$[1^{CF3}]. Yield: 44%. ^{1}H NMR (500 MHz, CD_3CN) δ 7.64 (d, *J* = 7.9 Hz, 8H), 7.09 (d, *J* = 7.9 Hz, 8H), 3.10 (q, *J* = 7.3 Hz, 16H), 1.25 – 1.07 (t, *J* = 7.3 Hz, 24H) ppm. ^{13}C NMR (126 MHz, CD_3CN) δ 156.87, 133.75, 124.27 (q, CF_3, *J* = 3.9 Hz), 118.30, 63.83 – 43.94 (m), 7.71 ppm. ^{19}F NMR (471 MHz, CD_3CN): δ 65.0 ppm. Anal. Calcd. for $C_{44}H_{56}F_{12}N_2S_4Zn$: C, 51.08; H, 5.46; N, 2.71. Found: C, 51.05; H, 4.98; N, 2.93.

Synthesis of tetraethylammonium tetra(*p*-toluenethiolato)cadmium salt ([Et$_4$N]$_2$[Cd(*p*-tolS)$_4$]. Under ambient conditions, a 20 mL scintillation vial equipped with a stir bar was charged with a solution of *p*-toluenethiol (1.24 g, 0.010 mol, 4 equiv), tetraethylammonium chloride (0.825 g, 0.005 mol, 2 equiv), and cadmium nitrate hexahydrate (0.771 g, 0.0025 mol, 1 equiv) in methanol (10 mL). While stirring, a solution of potassium hydroxide (0.561 g, 0.010 mol, 4 equiv)

in methanol (5 mL) was added dropwise and the mixture was allowed to stir at RT for 5 min. The reaction mixture was then stored at −30°C overnight. The resulting solid was filtered, washed with acetone and Et_2O, and dried in vacuo to give the desired product as pale blue crystals (1.2 g, 65%). ^{1}H NMR (400 MHz, CD_3CN) δ 7.33 (d, *J* = 8.0 Hz, 8H), 6.65 (d, *J* = 8.0 Hz, 8H), 3.10 (q, *J* = 7.3 Hz, 16H), 2.14 (s, 3H), 1.18 – 1.07 (t, *J* = 7.3 Hz 24H). ^{13}C NMR (101 MHz, CD_3CN) δ 134.00, 128.68, 118.28, 53.09, 20.81, 7.79. ^{113}Cd NMR (111 MHz, DMSO-d_6) δ 581.08.

NMR Spectra

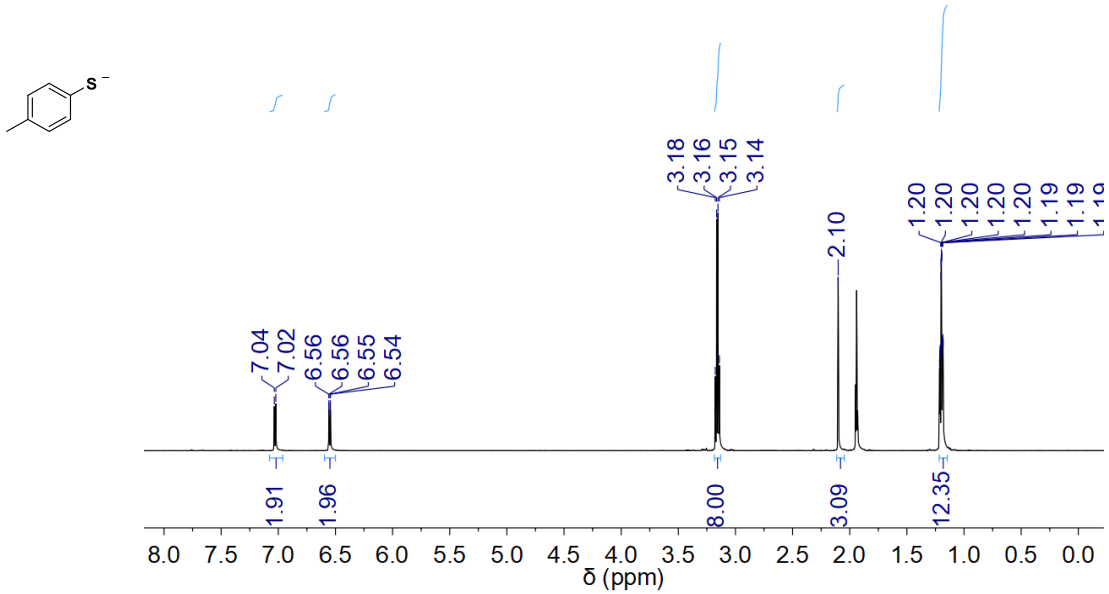

Figure S1. ^{1}H NMR spectrum of [Et_4N][**1^{Me}**] in CD_3CN at 20 °C.

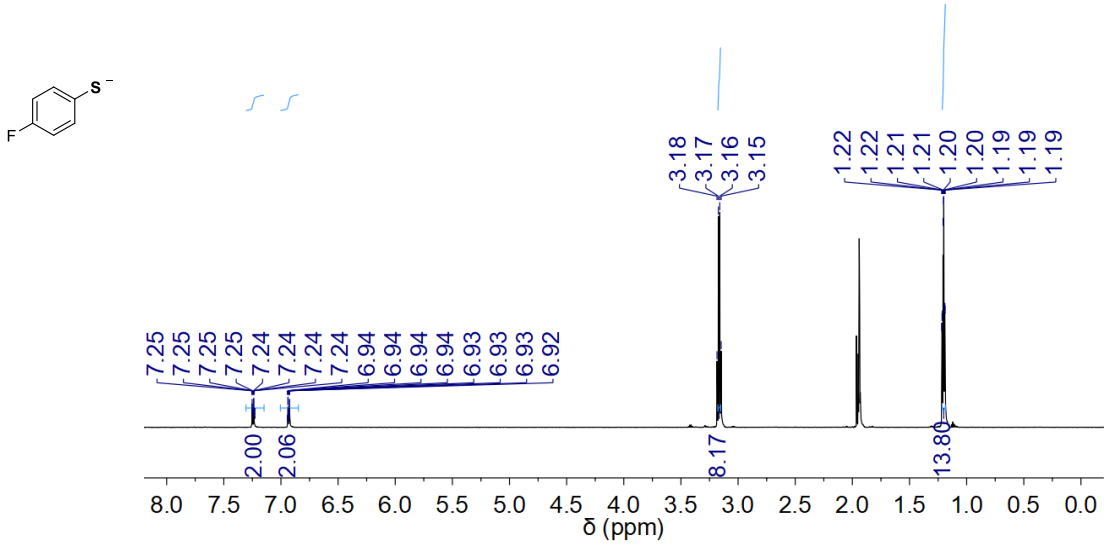

Figure S2. ^{1}H NMR spectrum of [Et_4N][**1^{F}**] in CD_3CN at 20 °C.

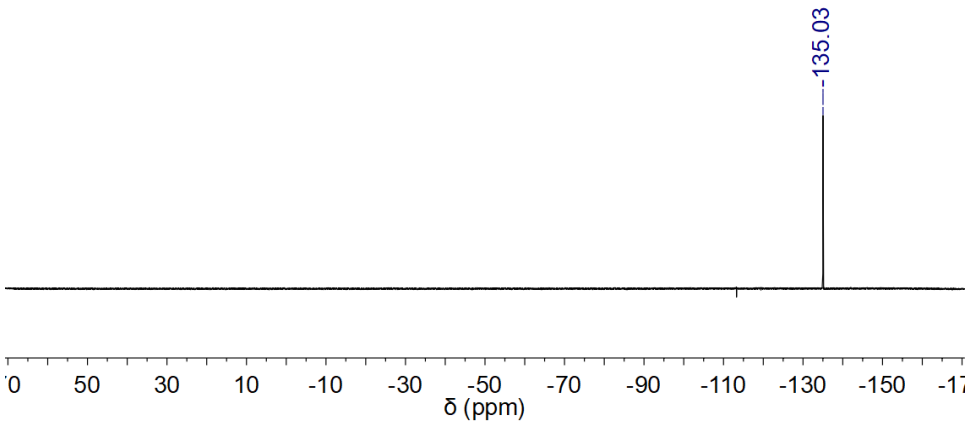

Figure S3. ^{19}F NMR spectrum of $[Et_4N][\mathbf{1^F}]$ in CD_3CN at 20 °C.

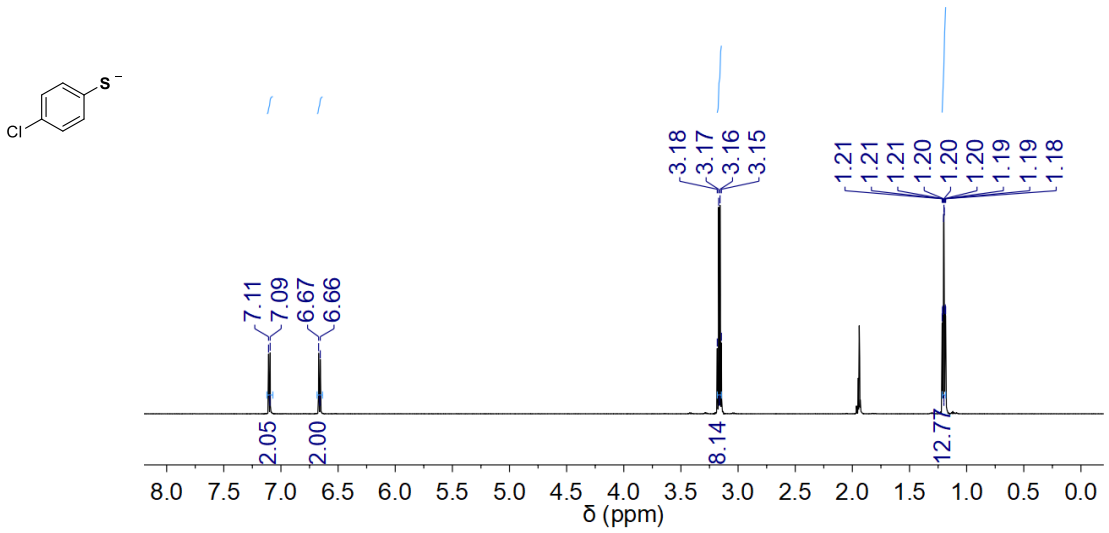

Figure S4. ^{1}H NMR spectrum of $[Et_4N][\mathbf{1^{Cl}}]$ in CD_3CN at 20 °C.

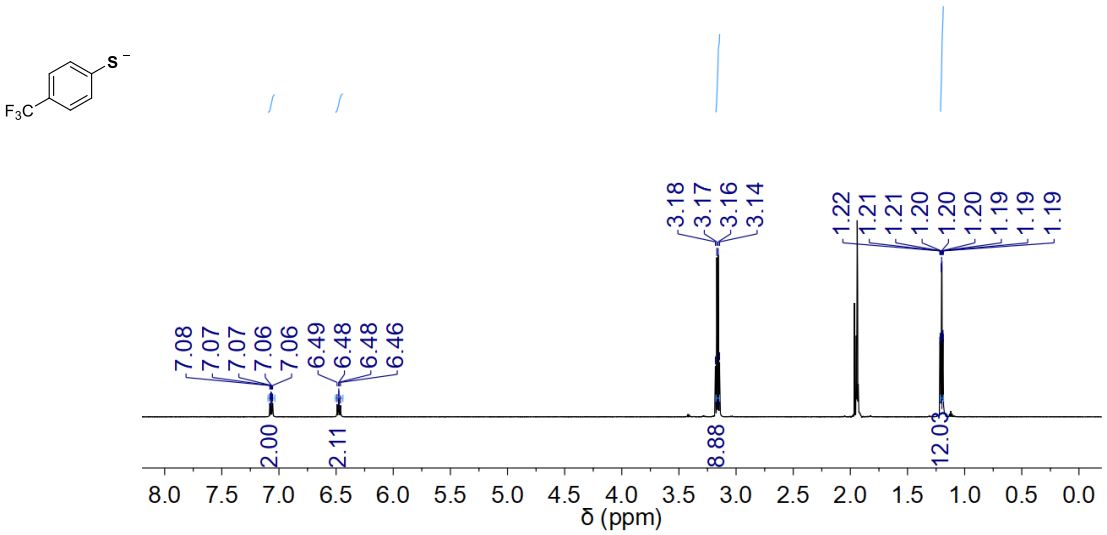

Figure S5. ^{1}H NMR spectrum of [Et_4N][**1**^{CF3}] in CD_3CN at 20 °C.

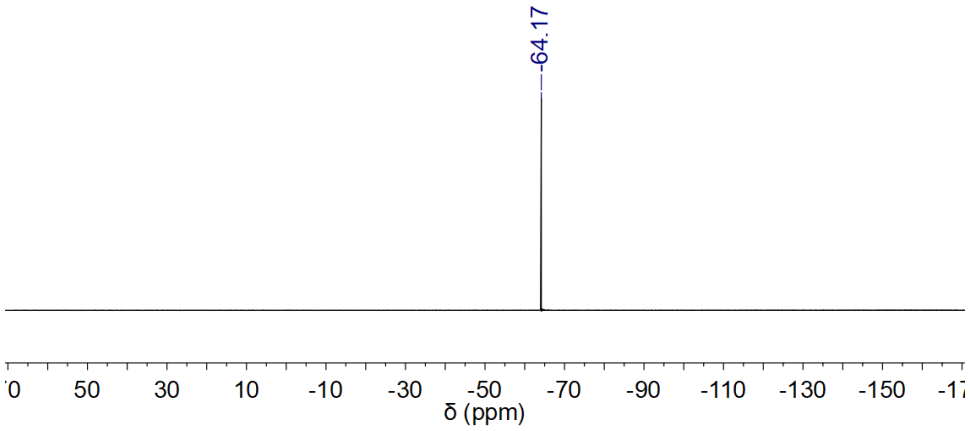

Figure S6. ^{19}F NMR spectrum of [Et_4N][**1**^{CF3}] in CD_3CN at 20 °C.

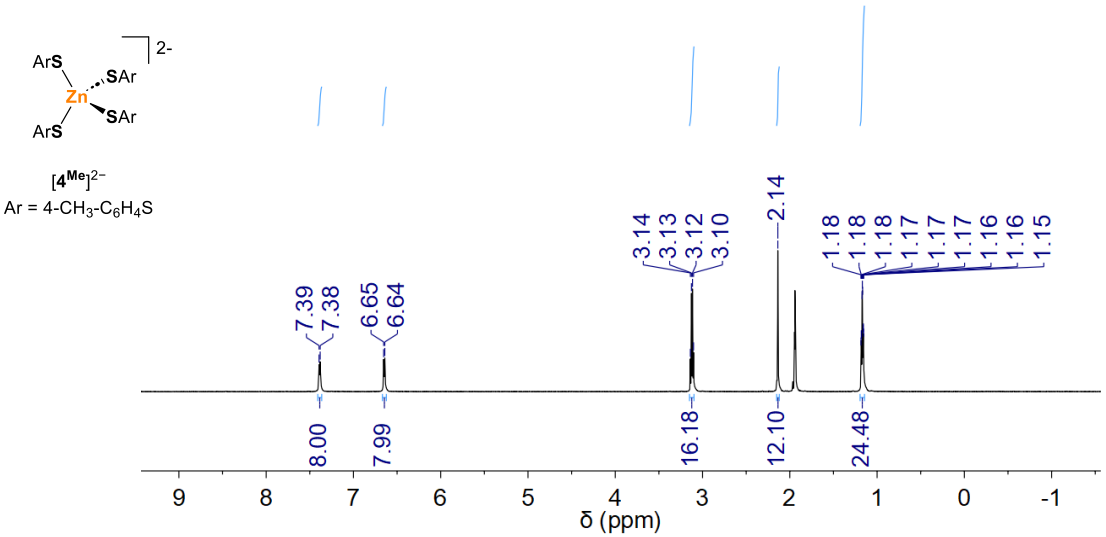

Figure S7. ^{1}H NMR spectrum of $[Et_4N]_2[\mathbf{4^{Me}}]$ in CD_3CN at 20 °C.

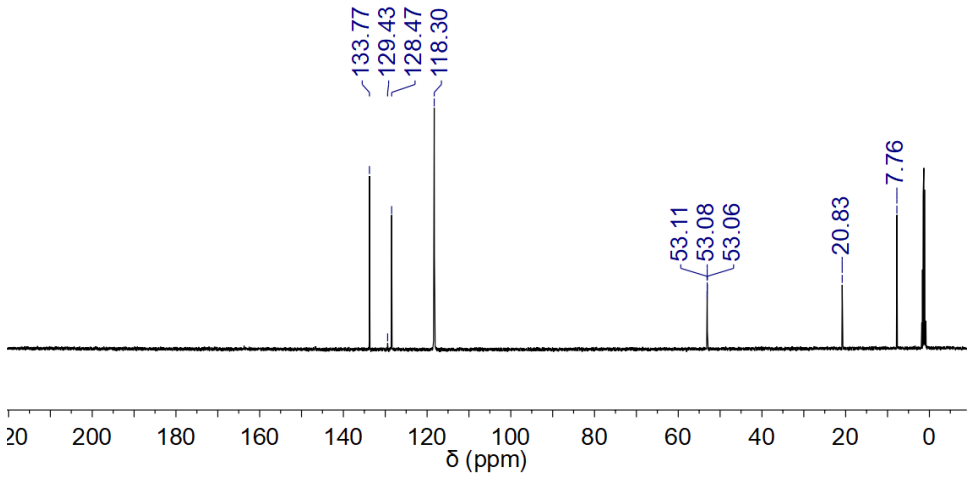

Figure S8. ^{13}C NMR spectrum of $[Et_4N]_2[\mathbf{4^{Me}}]$ in CD_3CN at 20 °C.

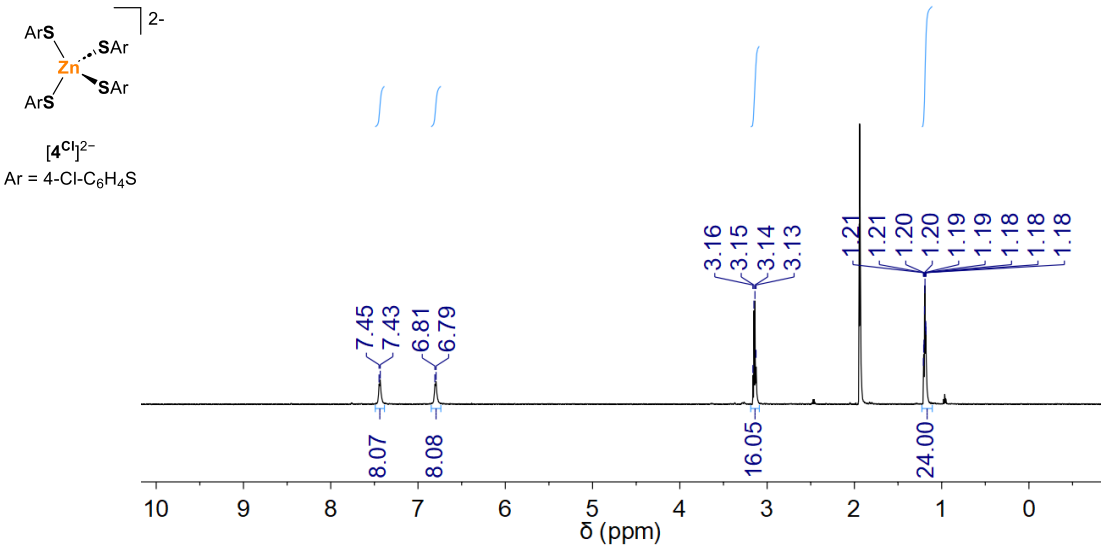

Figure S9. ^{1}H NMR spectrum of $[Et_4N]_2[\mathbf{4^{Cl}}]$ in CD_3CN at 20 °C.

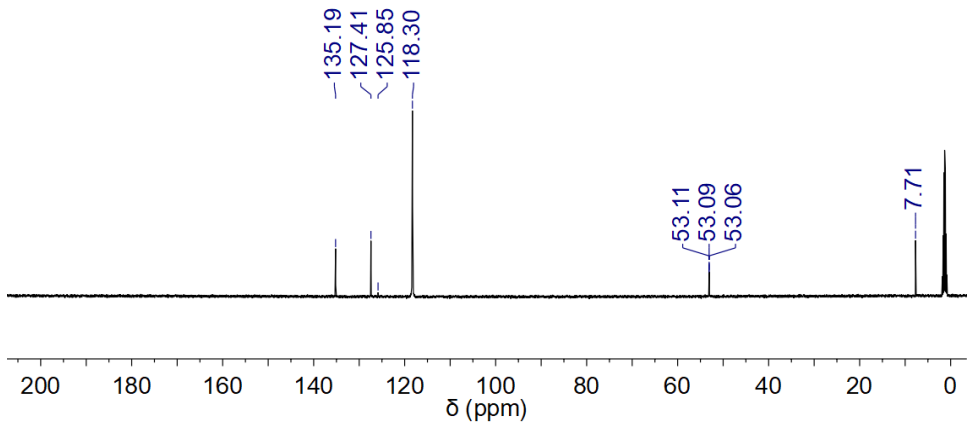

Figure S10. ^{13}C NMR spectrum of $[Et_4N]_2[\mathbf{4^{Cl}}]$ in CD_3CN at 20 °C.

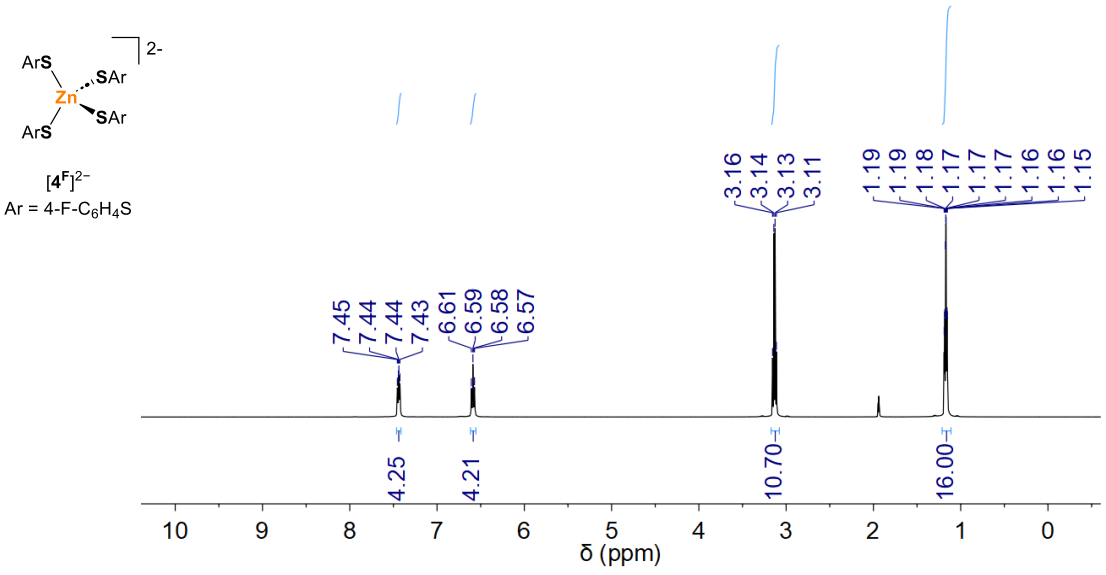

Figure S11. ^{1}H NMR spectrum of $[Et_4N]_2[\mathbf{4^F}]$ in CD_3CN at 20 °C.

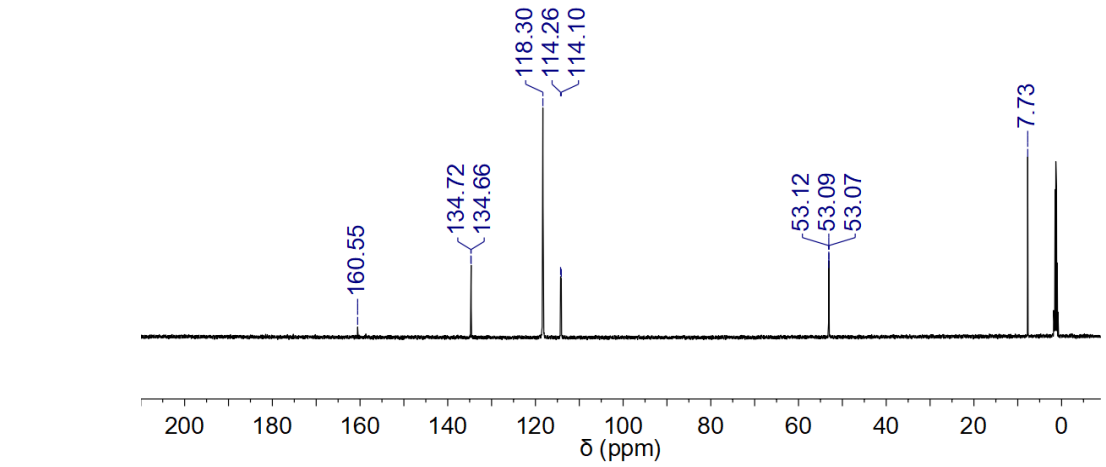

Figure S12. ^{13}C NMR spectrum of $[Et_4N]_2[\mathbf{4^F}]$ in CD_3CN at 20 °C.

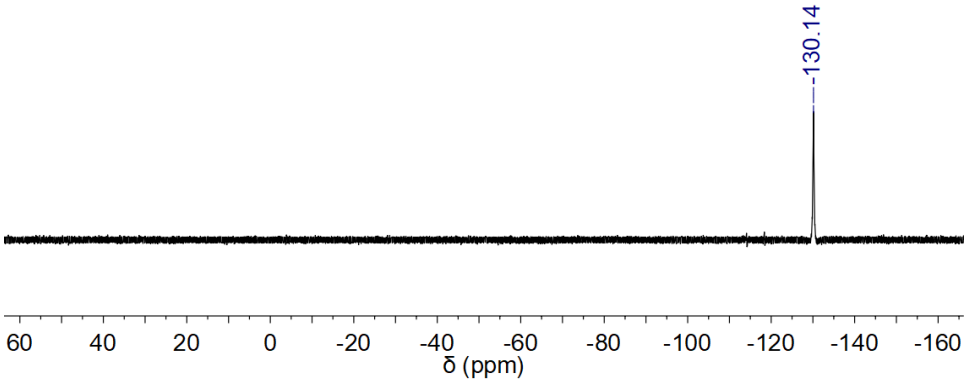

Figure S13. ^{19}F NMR spectrum of $[Et_4N]_2[\mathbf{4^F}]$ in CD_3CN at 20 °C.

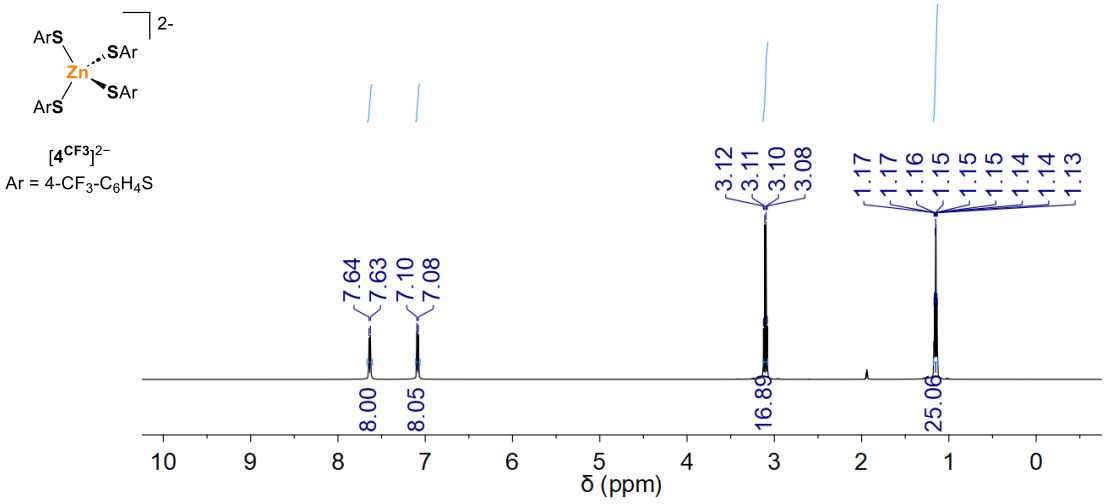

Figure S14. ^{1}H NMR spectrum of $[Et_4N]_2[\mathbf{4^{CF3}}]$ in CD_3CN at 20 °C.

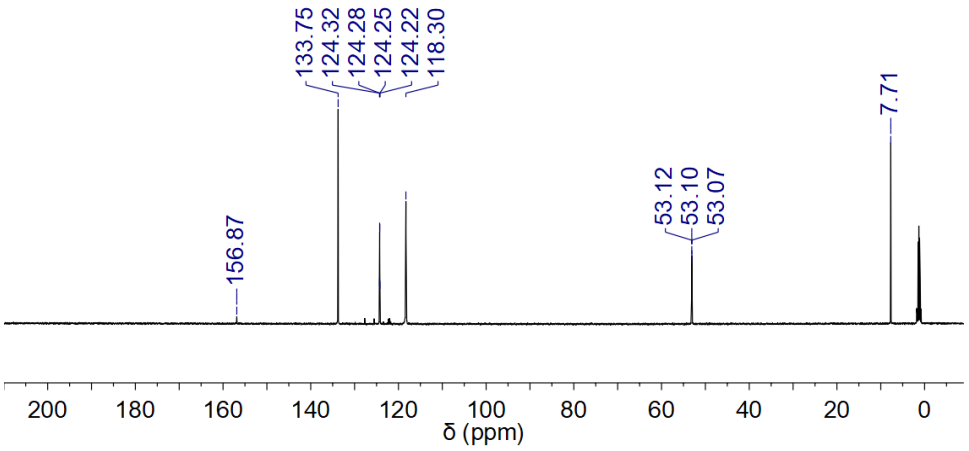

Figure S15. ^{13}C NMR spectrum of $[Et_4N]_2[\mathbf{4^{CF3}}]$ in CD_3CN at 20 °C.

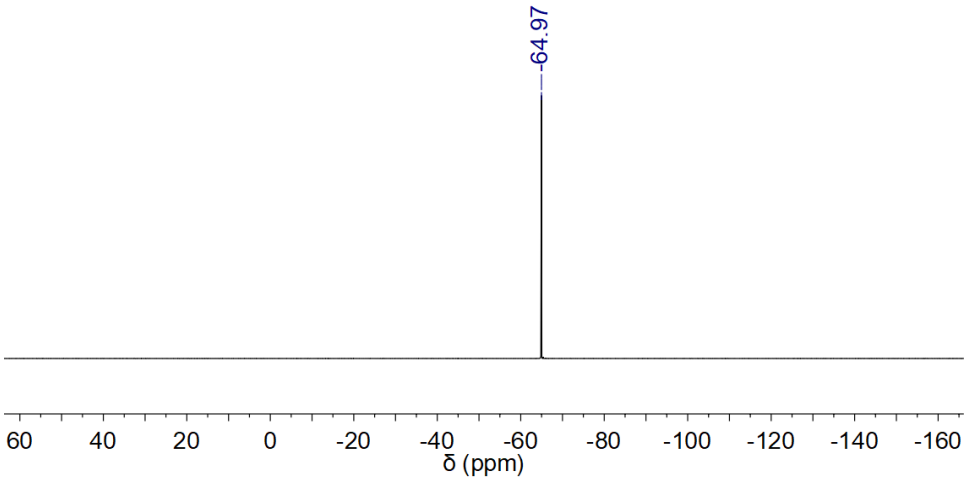

Figure S16. ^{19}F NMR spectrum of $[Et_4N]_2[\mathbf{4^{CF3}}]$ in CD_3CN at 20 °C.

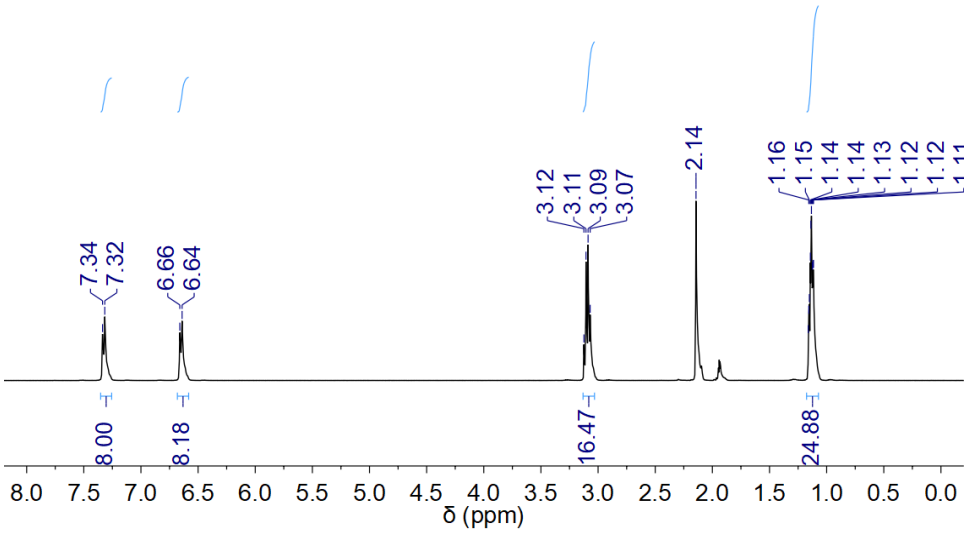

Figure S17. ^{1}H NMR spectrum of $[Et_4N]_2[Cd(p\text{-tolS})_4]$ in CD_3CN at 20 °C.

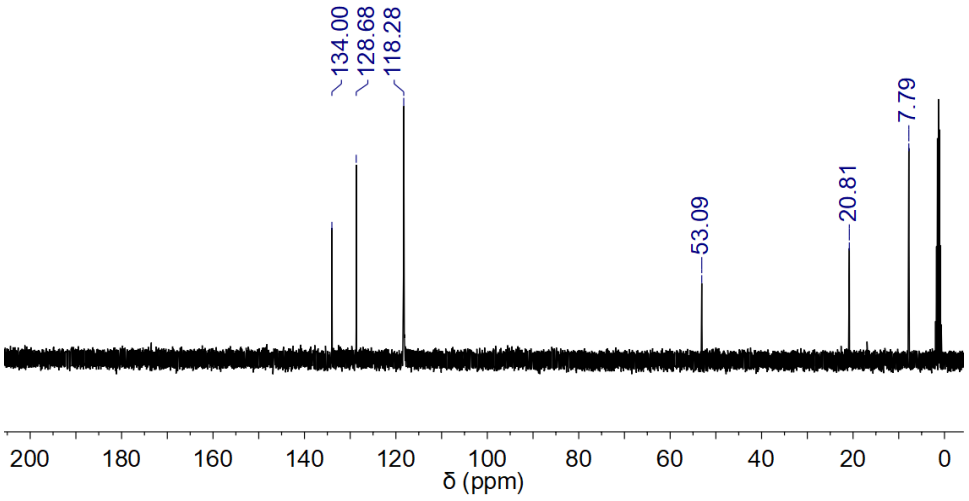

Figure S18. ^{13}C NMR spectrum of $[Et_4N]_2[Cd(p\text{-tolS})_4]$ in CD_3CN at 20 °C.

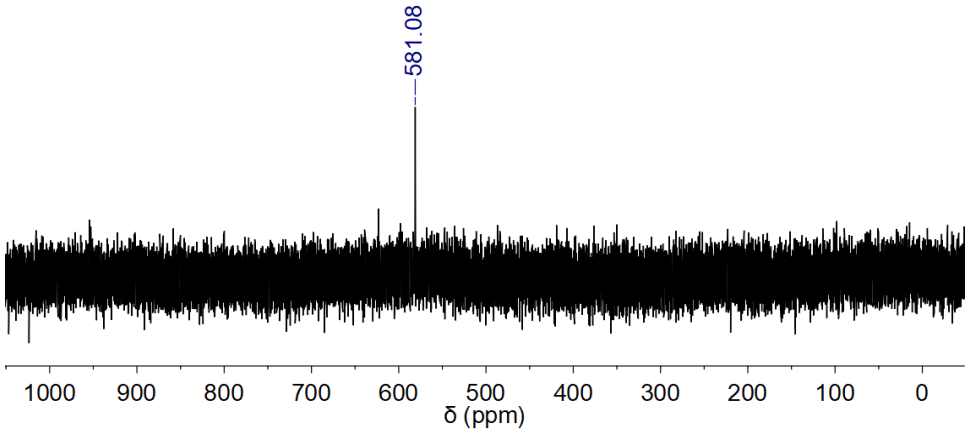

Figure S19. ^{113}Cd NMR spectrum of $[Et_4N]_2[Cd(p\text{-tolS})_4]$ in CD_3CN at 20 °C.

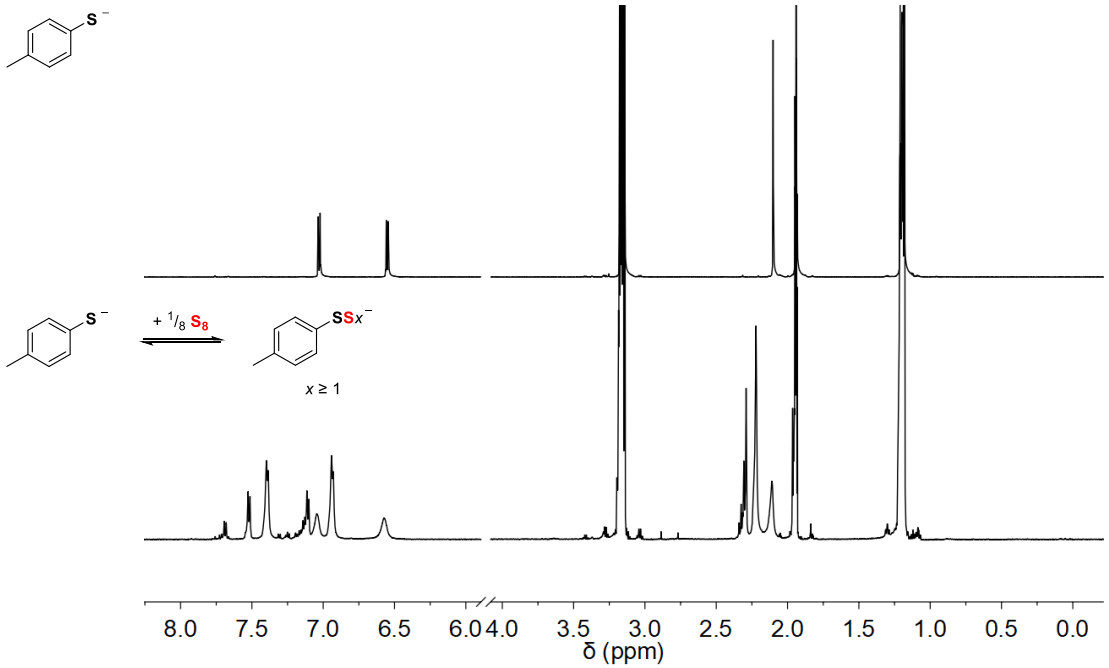

Figure S20. ^{1}H NMR spectra of $[Et_4N][\mathbf{1^{Me}}]$ (top) and $[Et_4N][\mathbf{1^{Me}}]$ treated with 1/8 equiv S_8 (bottom) in CD_3CN at 20 °C.

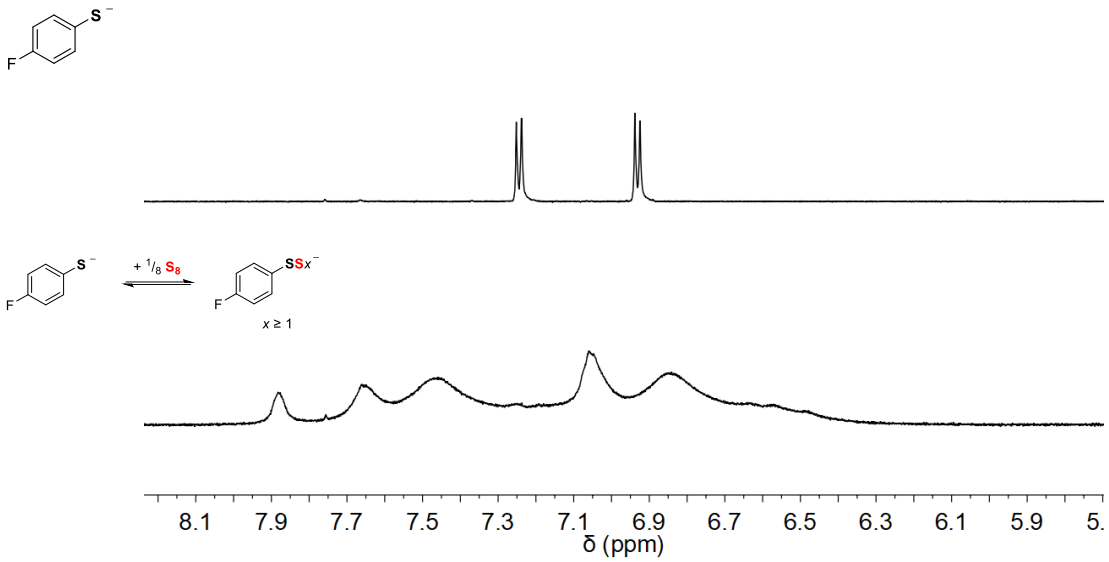

Figure S21. ^{1}H NMR spectra of [Et$_4$N][**1^{F}**] (top) and [Et$_4$N][**1^{F}**] treated with 1/8 equiv S$_8$ (bottom) in CD$_3$CN at 20 °C. Only the aromatic region is shown for clarity.

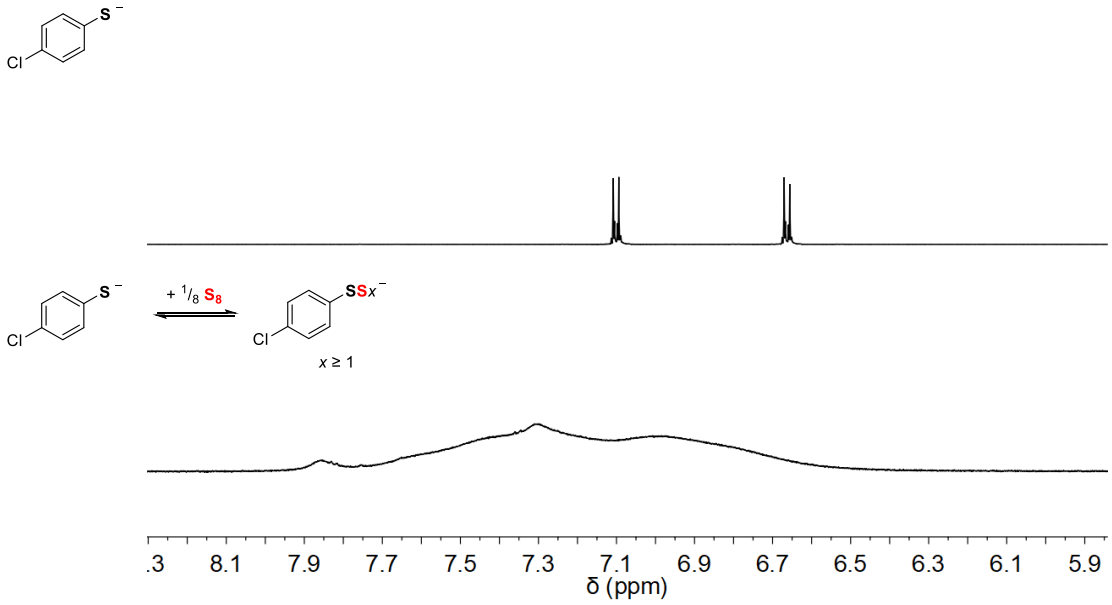

Figure S22. ^{1}H NMR spectra of [Et$_4$N][**1^{Cl}**] (top) and [Et$_4$N][**1^{Cl}**] treated with 1/8 equiv S$_8$ (bottom) in CD$_3$CN at 20 °C.

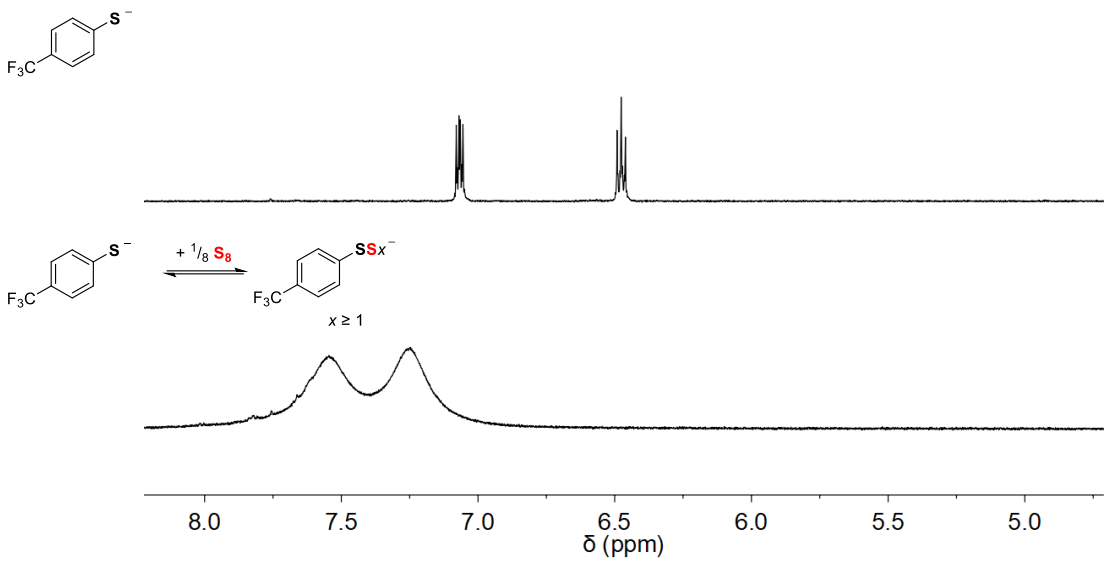

Figure S23. ^{1}H NMR spectra of [Et_4N][**1**^{CF3}] (top) and [Et_4N][**1**^{CF3}] treated with 1/8 equiv S_8 (bottom) in CD_3CN at 20 °C.

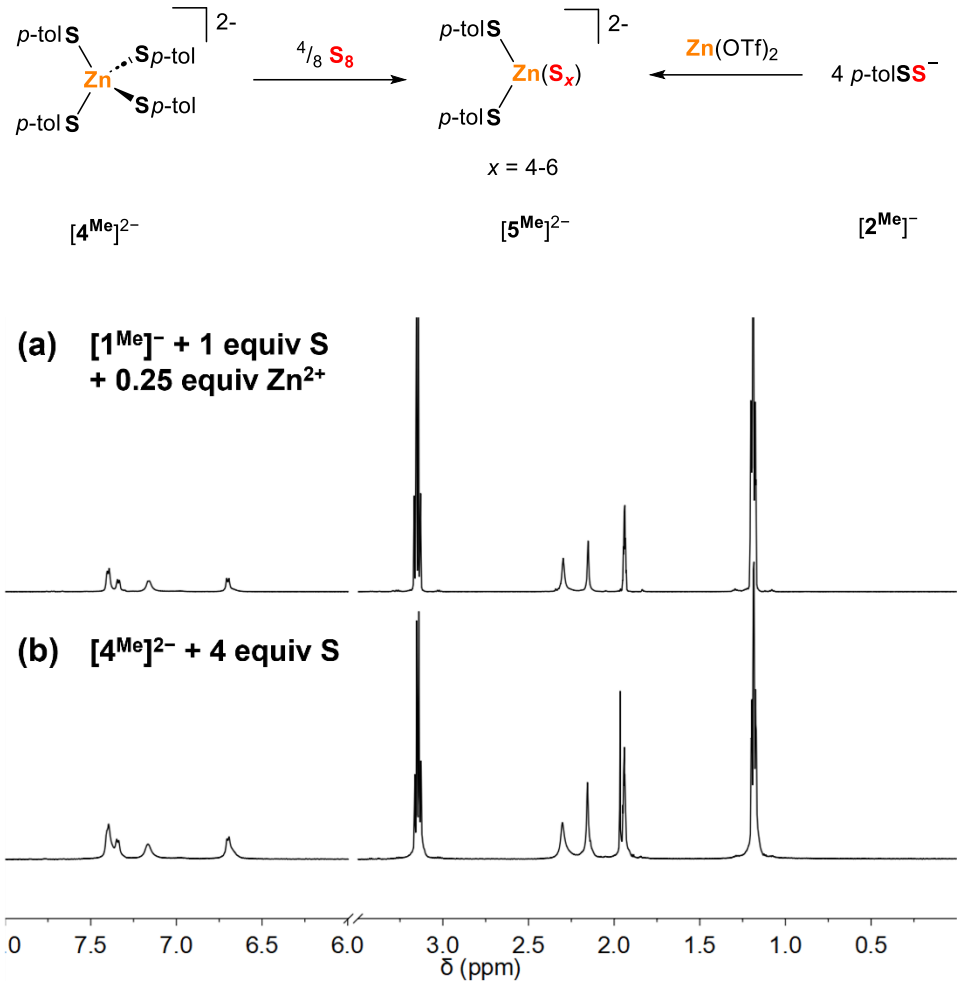

Figure S24. ^{1}H NMR spectra of $[Et_4N]_2[\mathbf{5^{Me}}]$ prepared by (a) treating a mixture of $[Et_4N][\mathbf{1^{Me}}]$ and 1/8 equiv S_8 with 0.25 equiv $Zn(OTf)_2$ or (b) treating $[Et_4N]_2[\mathbf{4^{Me}}]$ with 4/8 equiv S_8 in CD_3CN at 20 °C.

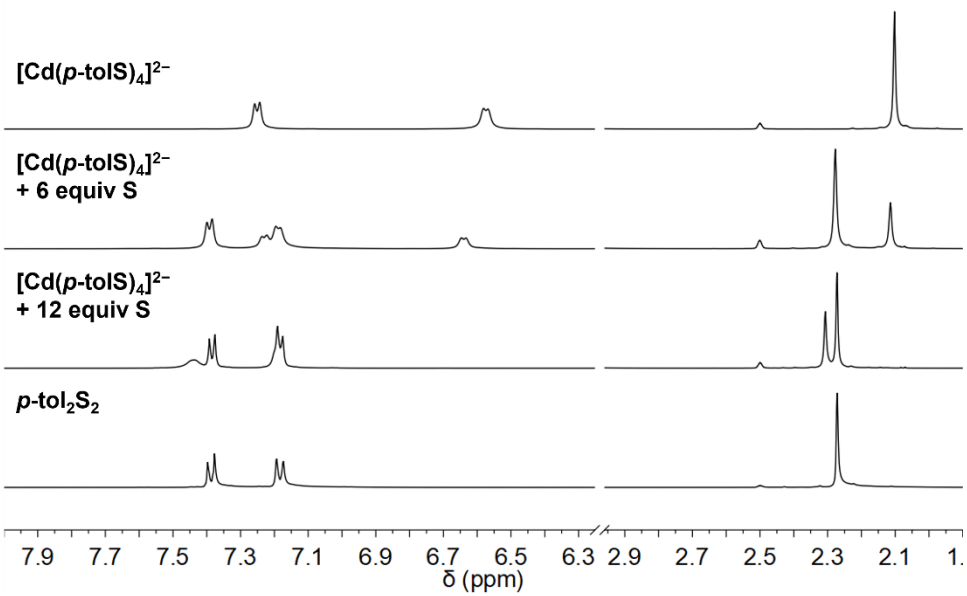

Figure S25. ^{1}H NMR spectra of $[Et_4N]_2[Cd(p\text{-tolS})_4]$ treated with increasing equiv S_8 in DMSO-d_6 at 20 °C.

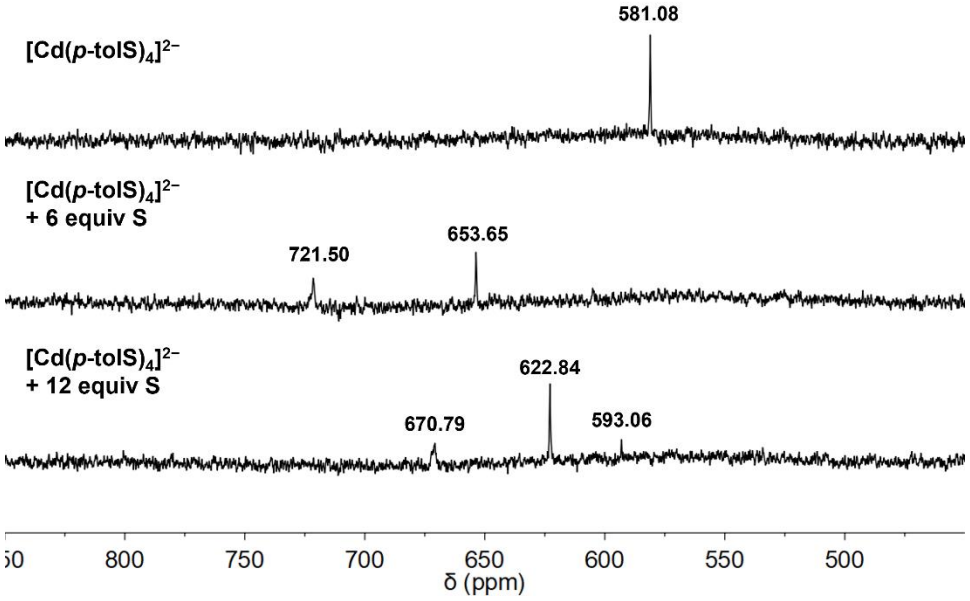

Figure S26. ^{113}Cd NMR spectra of $[Et_4N]_2[Cd(p\text{-tolS})_4]$ treated with increasing equiv S_8 in DMSO-d_6 at 20 °C.

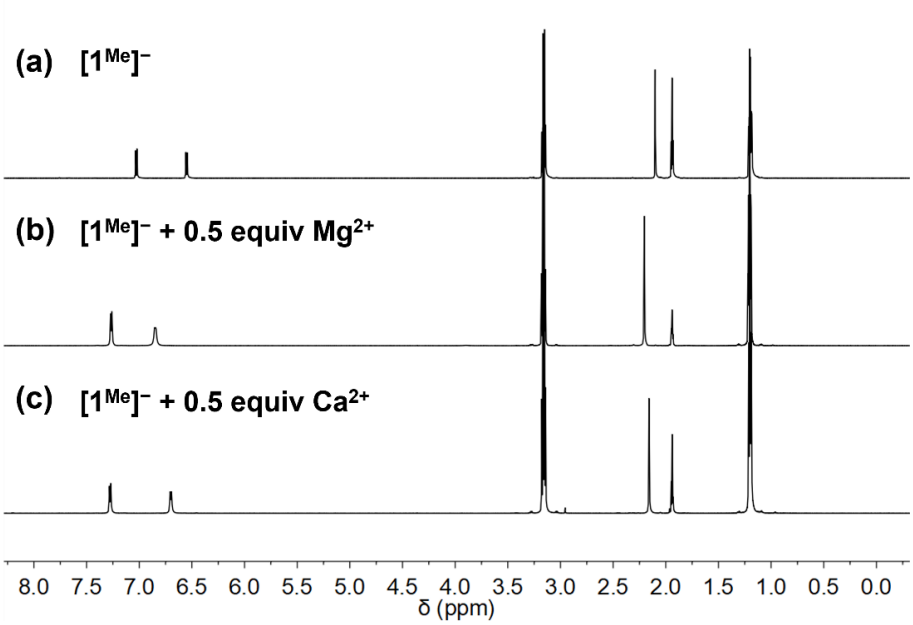

Figure S27. ^{1}H NMR spectra of (a) [Et_4N][**1^{Me}**] treated with (b) 0.5 equiv $Mg(ClO_4)_2$ or (c) 0.5 equiv $Ca(OTf)_2$ in CD_3CN at 20 °C.

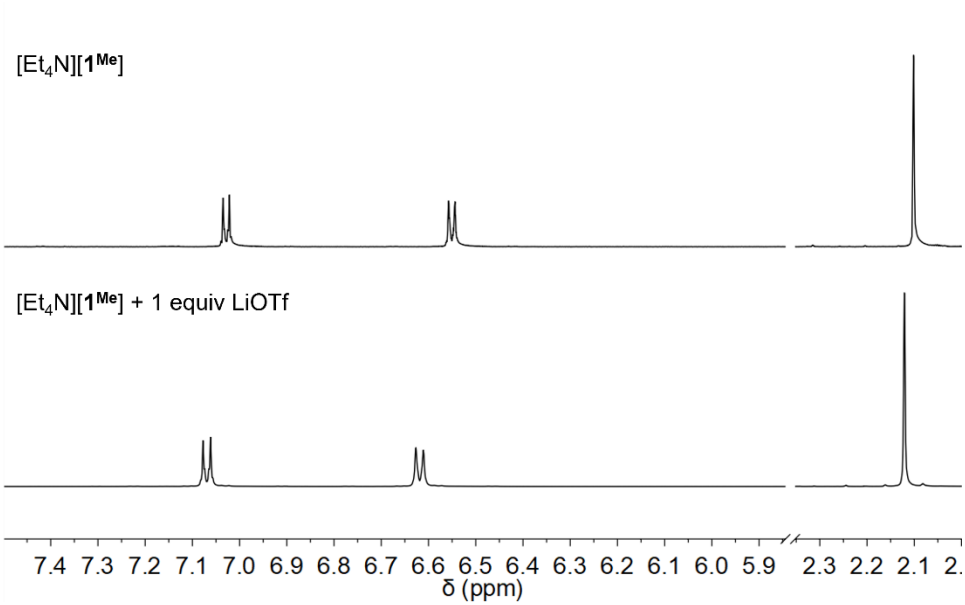

Figure S28. ^{1}H NMR spectrum of [Et_4N][**1^{Me}**] treated with 1 equiv LiOTf in CD_3CN at 20 °C.

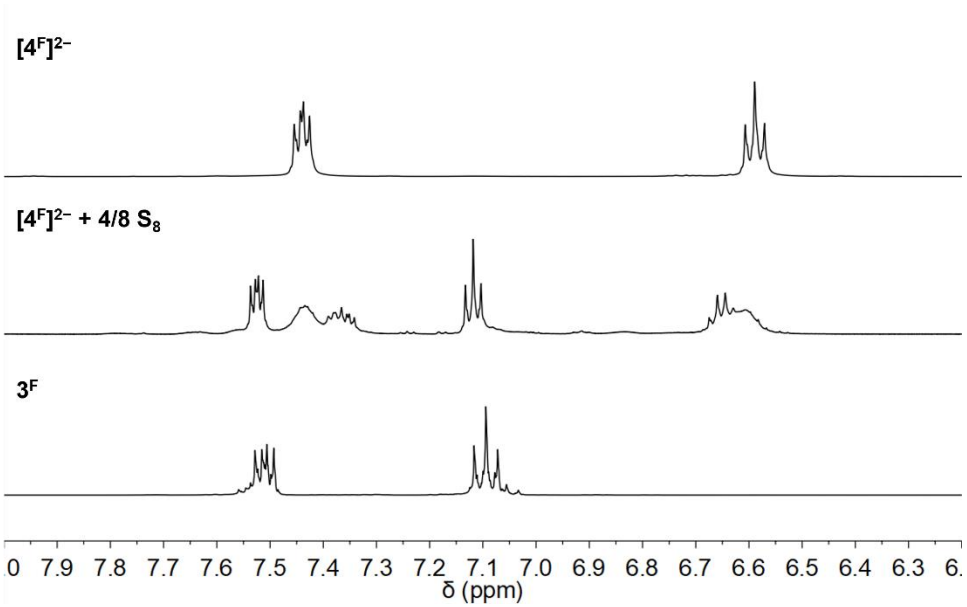

Figure S29. ^{1}H NMR spectra of $[Et_4N]_2$[**4^{F}**] treated with 4/8 S_8 in CD_3CN at 20 °C.

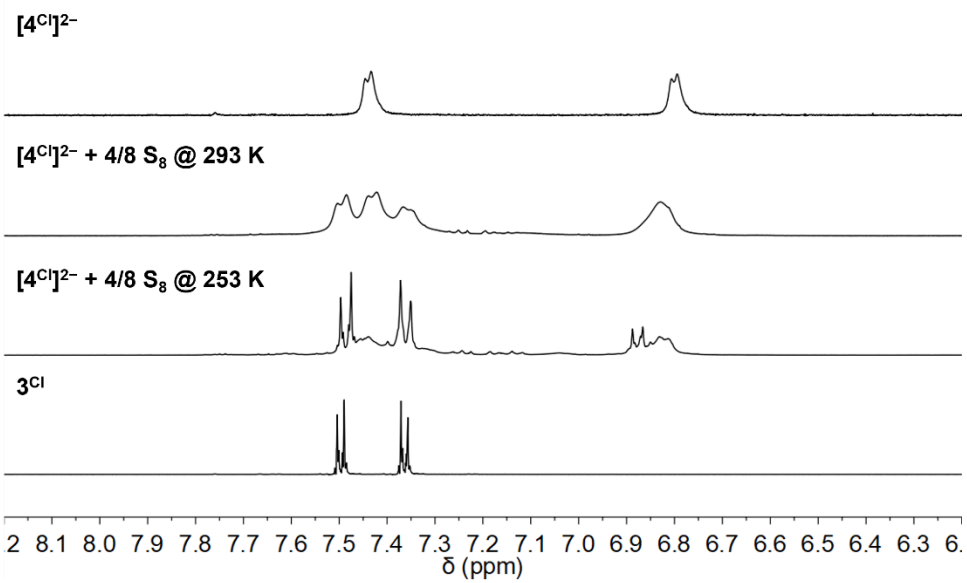

Figure S30. ^{1}H NMR spectra of $[Et_4N]_2$[**4^{Cl}**] treated with 4/8 S_8 in CD_3CN at 20 and −20 °C.

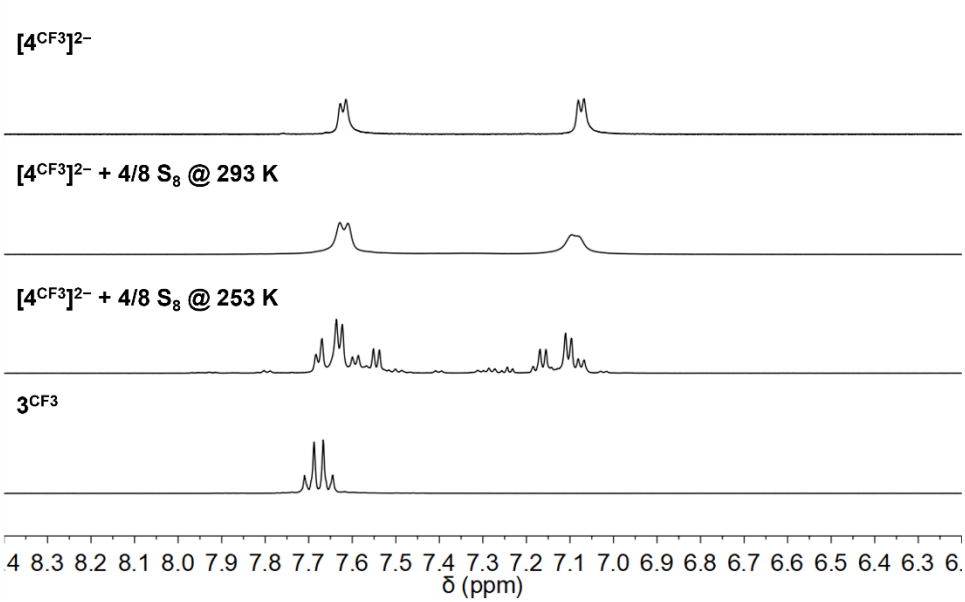

Figure S31. ^{1}H NMR spectra of $[Et_4N]_2[\mathbf{4^{CF3}}]$ treated with 4/8 S_8 in CD_3CN at 20 and −20 °C.

General methodology for metal triflate salt addition to p-tolyl thiolate/polysulfanide mixtures

To CH_3CN solutions of $[Et_4N][\mathbf{1^{Me}}]$ (0.010 g in 1.0 mL) was added a saturated S_8 solution in toluene (0.039 M, 12.6 μL, 1 equiv S). To this mixture was added increasing amounts of metal triflate salt solutions in CH_3CN (up to 1 equiv metal triflate in 1.0 mL), then the reaction mixture was concentrated in vacuo. These residues were redissolved in CD_3CN (0.4 mL) and transferred to NMR tubes for analysis.

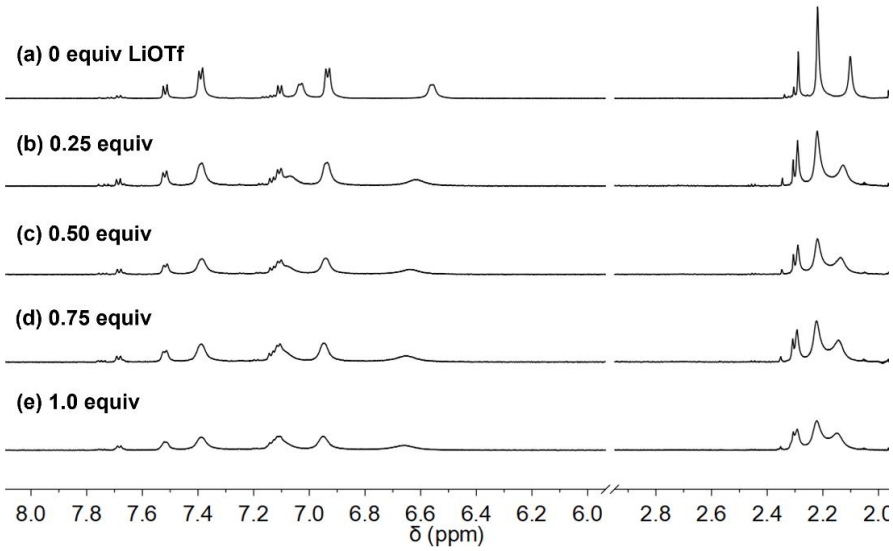

Figure S32. ^{1}H NMR spectra of a CD_3CN solution of $[Et_4N][\mathbf{1^{Me}}]$ treated with 1/8 equiv S_8 with (a) no added LiOTf, (b) 0.25 equiv LiOTf, (c) 0.50 equiv LiOTf, (d) 0.75 equiv LiOTf, and (e) 1.0 equiv LiOTf at 20 °C.

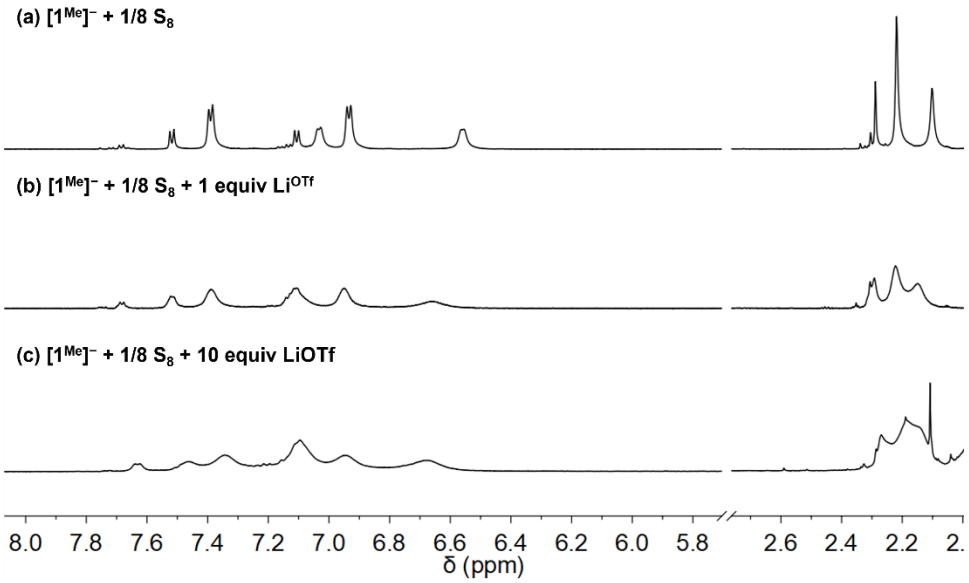

Figure S33. ^{1}H NMR spectra of (a) [Et$_4$N][**1^{Me}**] treated with 1/8 equiv S_8, (b) the same solution with 1 equiv LiOTf added, and (c) the same solution with 10 equiv LiOTf added in CD_3CN at 20 °C.

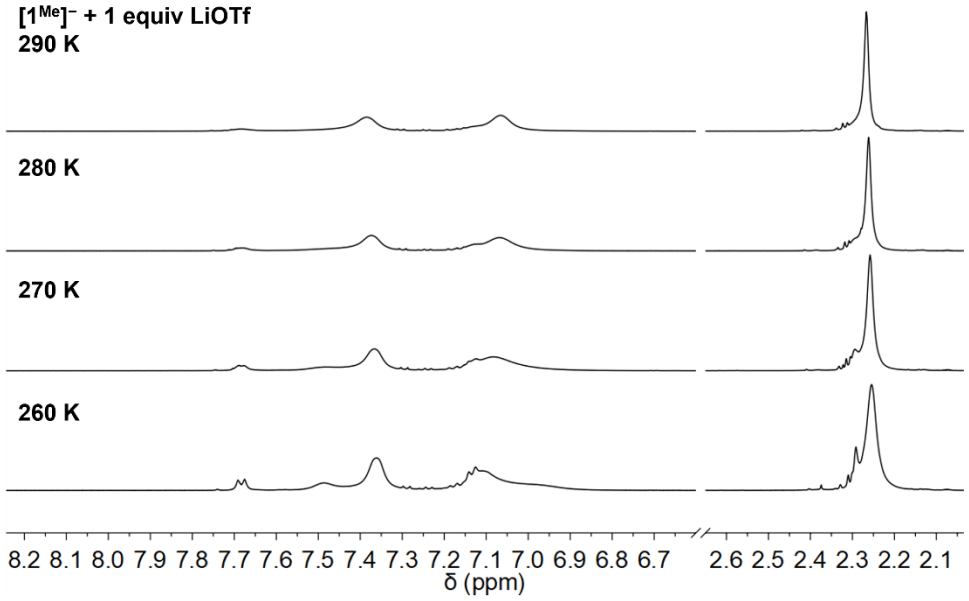

Figure S34. ^{1}H NMR spectra stack of [Et$_4$N][**1^{Me}**] treated with 1/8 equiv S_8 and 1 equiv LiOTf in CD_3CN showing resolution of higher-order polysulfanide peaks upon cooling from 290 K to 260 K.

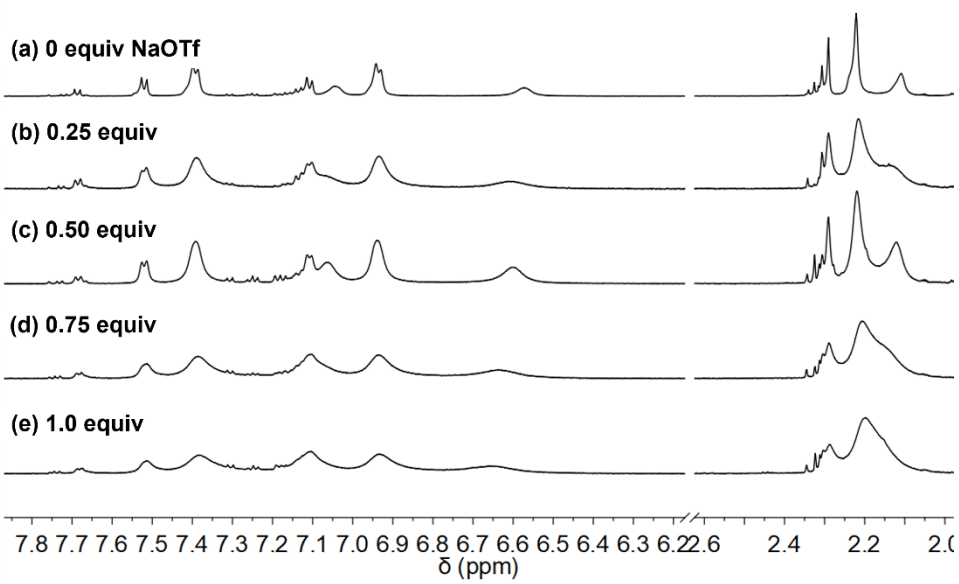

Figure S35. ^{1}H NMR spectra of (a) [Et_4N][**1^{Me}**] treated with 1/8 equiv S_8, (b) the same solution with 0.25 equiv NaOTf, (c) the same solution with 0.50 equiv NaOTf, (d) the same solution with 0.75 equiv NaOTf, and (e) the same solution with 1.0 equiv NaOTf in CD_3CN at 20 °C.

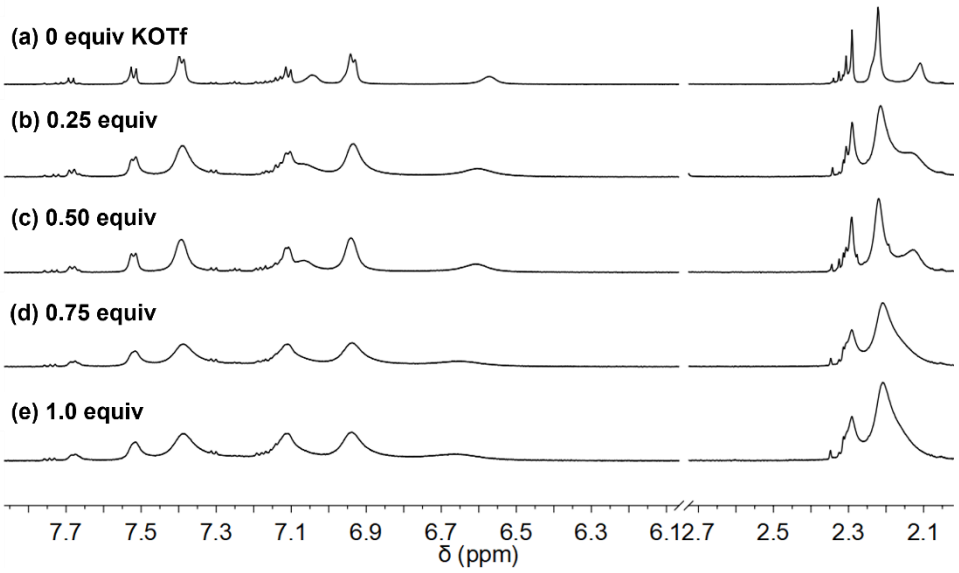

Figure S36. ^{1}H NMR spectra of (a) [Et_4N][**1^{Me}**] treated with 1/8 equiv S_8, (b) the same solution with 0.25 equiv KOTf, (c) the same solution with 0.50 equiv KOTf, (d) the same solution with 0.75 equiv KOTf, and (e) the same solution with 1.0 equiv KOTf in CD_3CN at 20 °C.

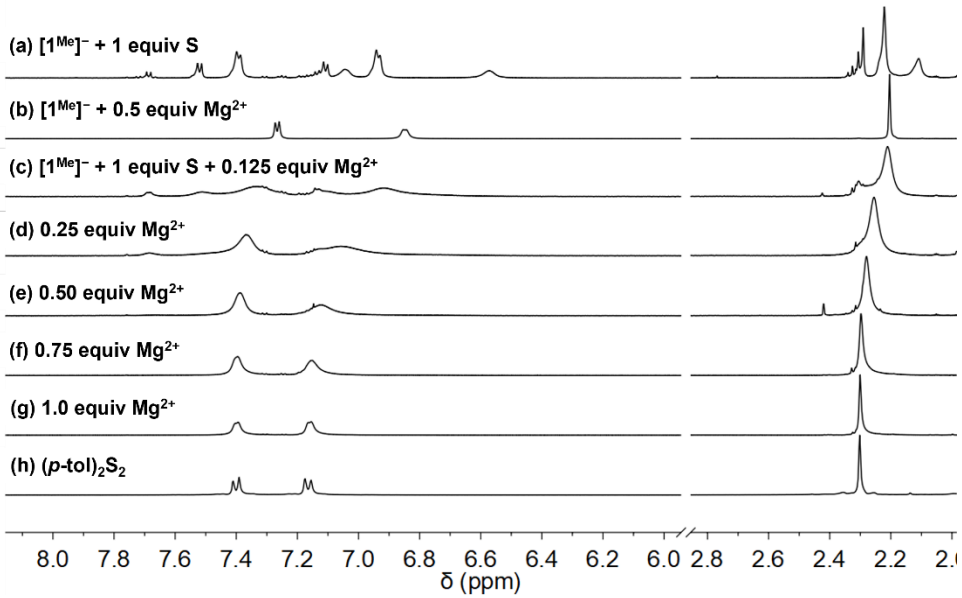

Figure S37. ^{1}H NMR spectra of (a) [Et_4N][**1**] treated with 1/8 equiv S_8, (b) [Et_4N][**1**] treated with 0.5 equiv $Mg(ClO_4)_2$, (c) [Et_4N][**1**] treated with 1/8 equiv S_8 and 0. 125 equiv $Mg(OTf)_2$, (d) the same solution with 0. 25 equiv $Mg(OTf)_2$, (e) the same solution with 0.50 equiv $Mg(OTf)_2$, (f) the same solution with 0.75 equiv $Mg(OTf)_2$, (f) the same solution with 1.0 equiv $Mg(OTf)_2$, and (h) (*p*-tol)$_2S_2$ in CD_3CN at 20 °C.

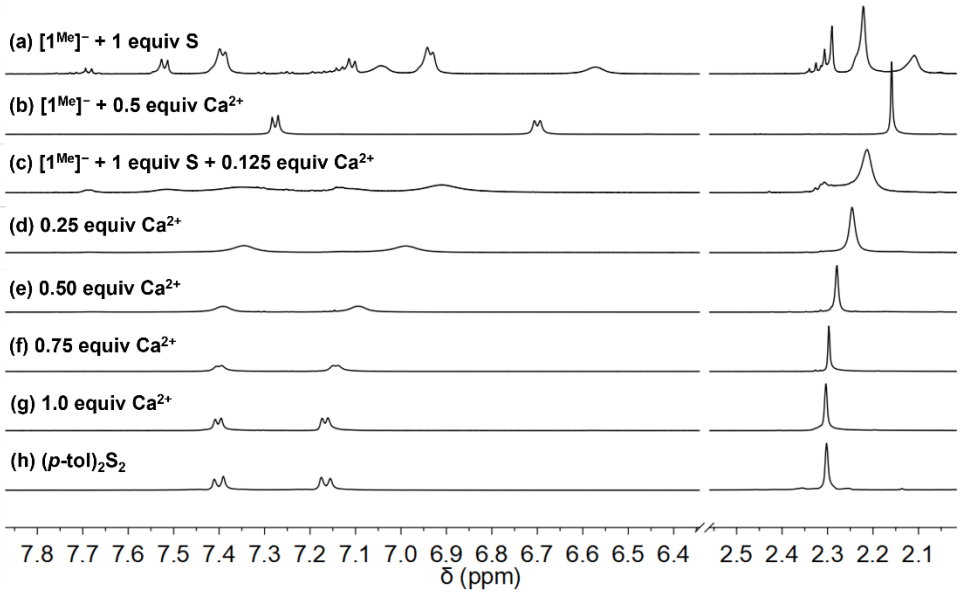

Figure S38. ^{1}H NMR spectra of (a) [Et_4N][**1^{Me}**] treated with 1/8 equiv S_8, (b) [Et_4N][**1**] treated with 0.5 equiv $Ca(OTf)_2$, (c) [Et_4N][**1**] treated with 1/8 equiv S_8 and 0. 125 equiv $Ca(OTf)_2$, (d) the same solution with 0. 25 equiv $Ca(OTf)_2$, (e) the same solution with 0.50 equiv $Ca(OTf)_2$, (f) the same solution with 0.75 equiv $Ca(OTf)_2$, (f) the same solution with 1.0 equiv $Ca(OTf)_2$, and (h) (*p*-tol)$_2S_2$ in CD_3CN at 20 °C.

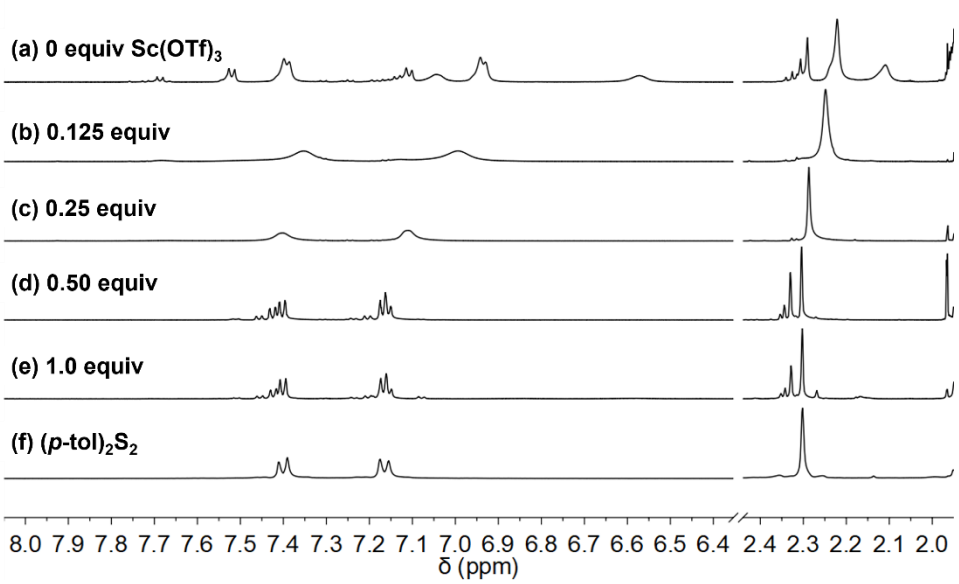

Figure S39. ^{1}H NMR spectra of (a) [Et$_4$N][**1^{Me}**] treated with 1/8 equiv S_8, (b) the same solution with 0.125 equiv Sc(OTf)$_3$, (c) the same solution with 0.25 equiv Sc(OTf)$_3$, (d) the same solution with 0.50 equiv Sc(OTf)$_3$, (e) the same solution with 1.0 Sc(OTf)$_3$, and (f) (*p*-tolS)$_2$S$_2$ in CD$_3$CN at 20 °C.

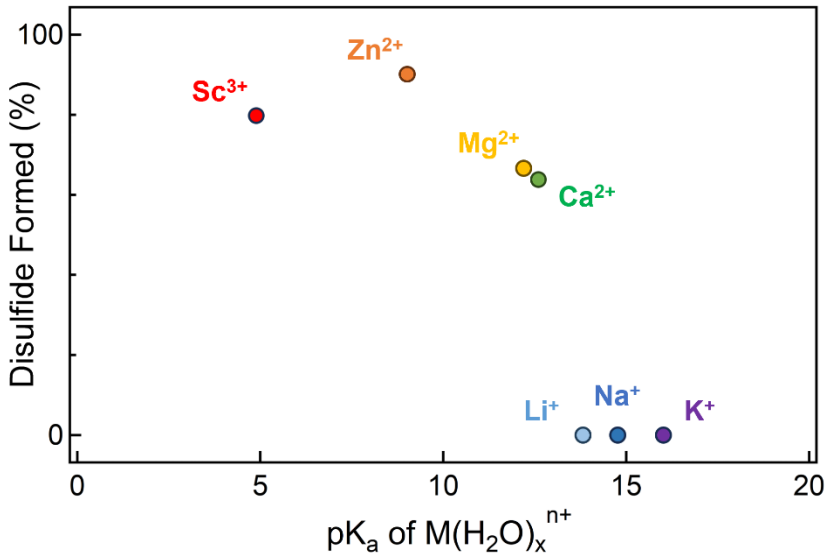

Figure S40. Comparison of **3^{Me}** formed from a mixture of [Et$_4$N][**1^{Me}**] + 1/8 equiv S_8 treated with 0.25 equiv M(OTf)$_n$ in CD$_3$CN (as measured by benzylic ^{1}H shift) vs. Lewis acidity of metal cation (as measured by pK_a of metal aquo complex).

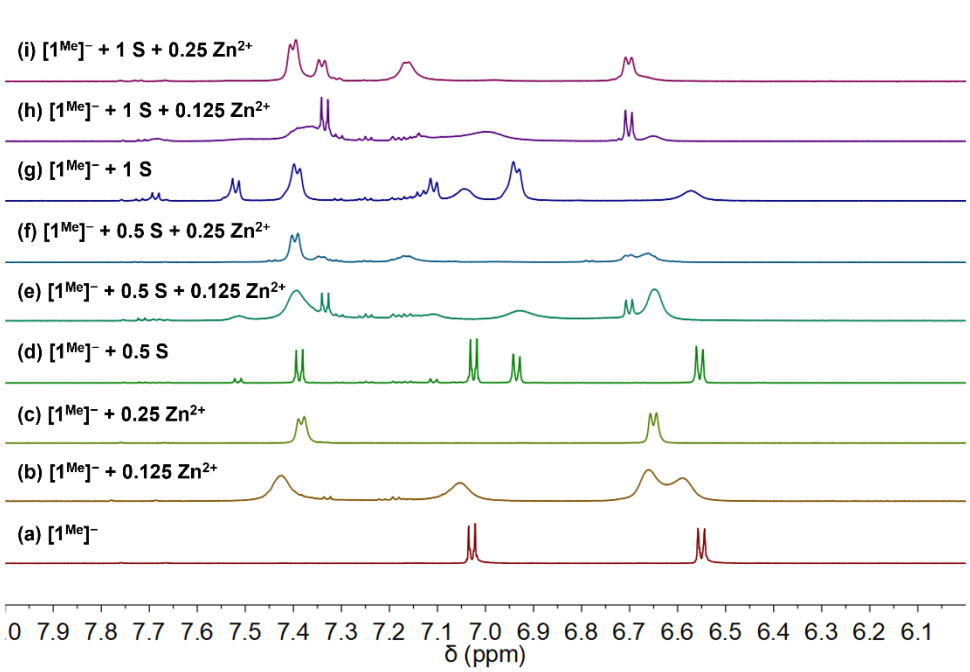

Figure S41. ^{1}H NMR spectra of (a) [Et$_4$N][**1^{Me}**] treated with (b) 0.125 equiv Zn(OTf)$_2$, (c) 0.25 equiv Zn(OTf)$_2$, (d) 0.5 equiv S, (e) 0.5 equiv S + 0.125 equiv Zn(OTf)$_2$, (f) 0.5 equiv S + 0.25 quiv Zn(OTf)$_2$, (g) 1 equiv S, (h) 1 equiv S + 0.125 equiv Zn(OTf)$_2$, (i) 1 equiv S + 0.25 equiv Zn(OTf)$_2$ in CD$_3$CN at 20 °C.

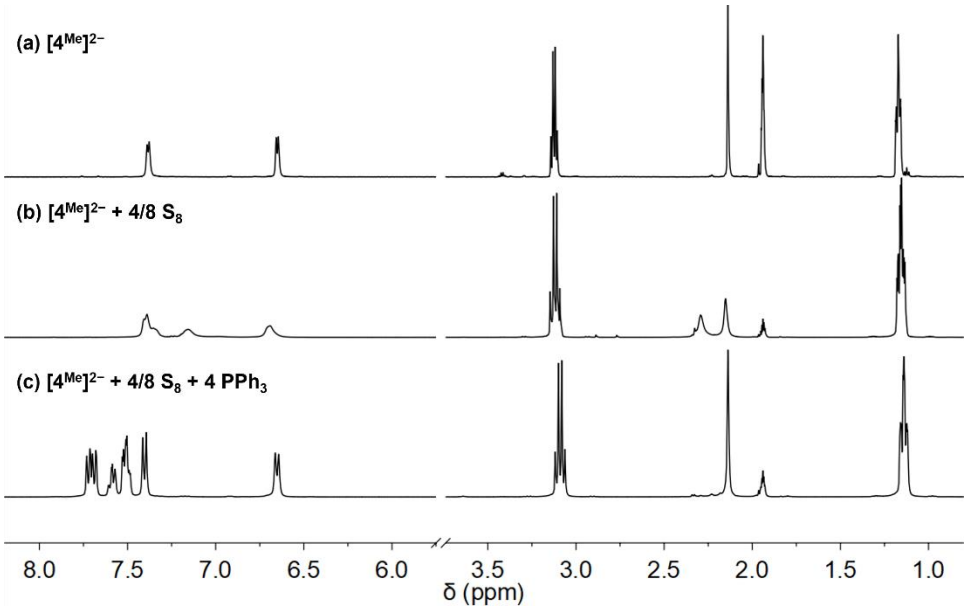

Figure S42. ^{1}H NMR spectra of (a) [Et$_4$N]$_2$[**4^{Me}**] treated with (b) S$_8$ (4 equiv S), then with (c) PPh$_3$ (4 equiv) in CD$_3$CN at 20 °C.

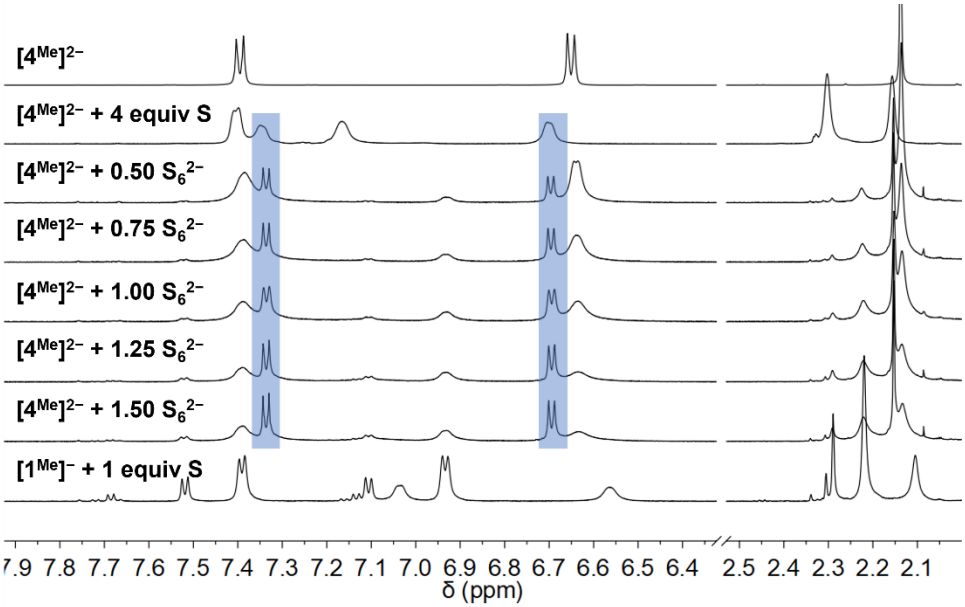

Figure S43. ^{1}H NMR spectra of $[Et_4N]_2[\mathbf{4^{Me}}]$ treated with increasing equiv $[TBA]_2[S_6]$ in CD_3CN at 20 °C. Peaks corresponding to $[\mathbf{5^{Me}}]^{2-}$ are highlighted.

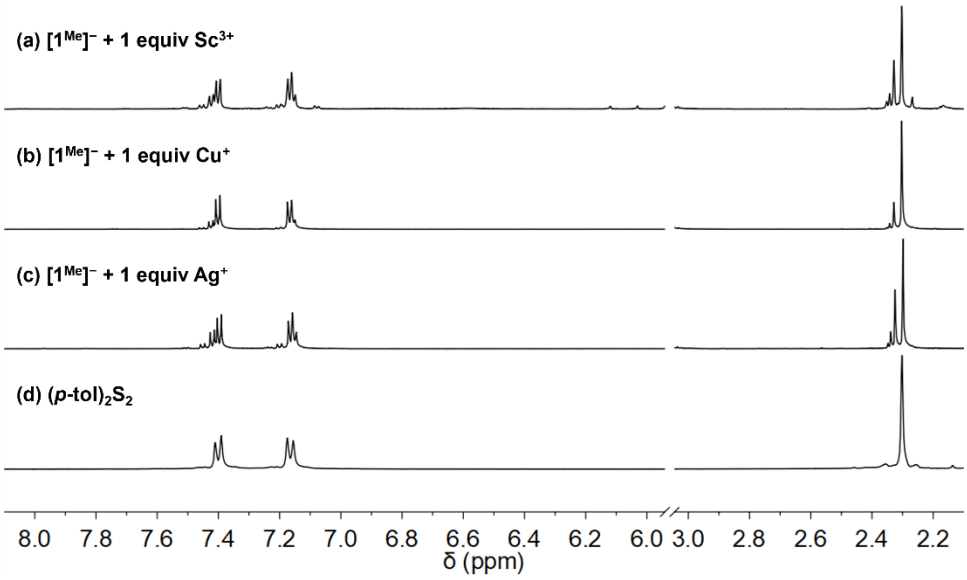

Figure S44. ^{1}H NMR spectra of $[Et_4N][\mathbf{1^{Me}}]$ treated with (a) 1 equiv $Sc(OTf)_3$, (b) 1 equiv $(CH_3CN)_4CuPF_6$, and (c) 1equiv Ag(OTf) in comparison to (d) $(p\text{-tol})_2S_2$ in CD_3CN at 20 °C.

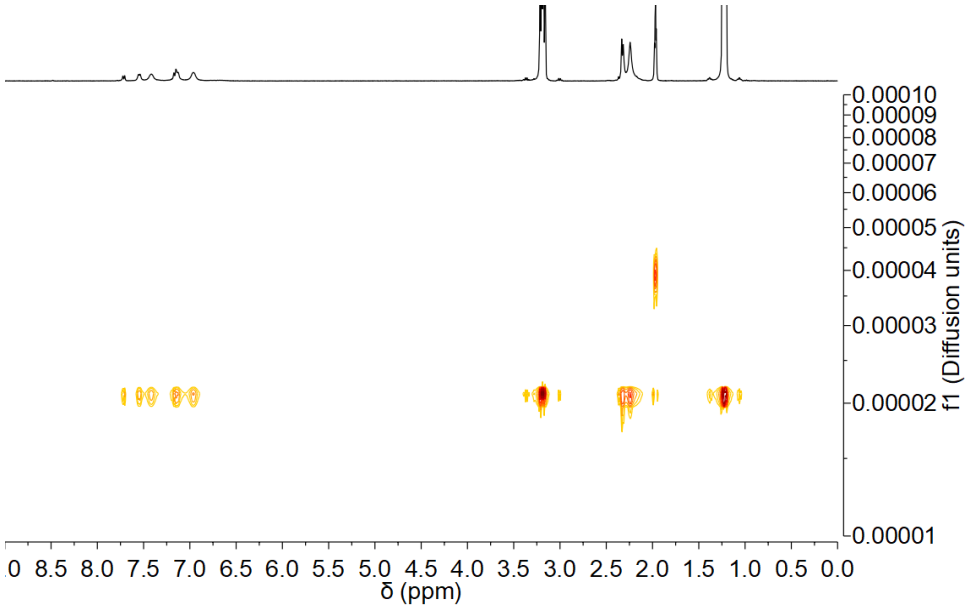

Figure S45. 2D ^{1}H DOSY plot of [Et_4N][**1^{Me}**] treated with S_8 (1 S atom equiv) in CD_3CN at 20° C.

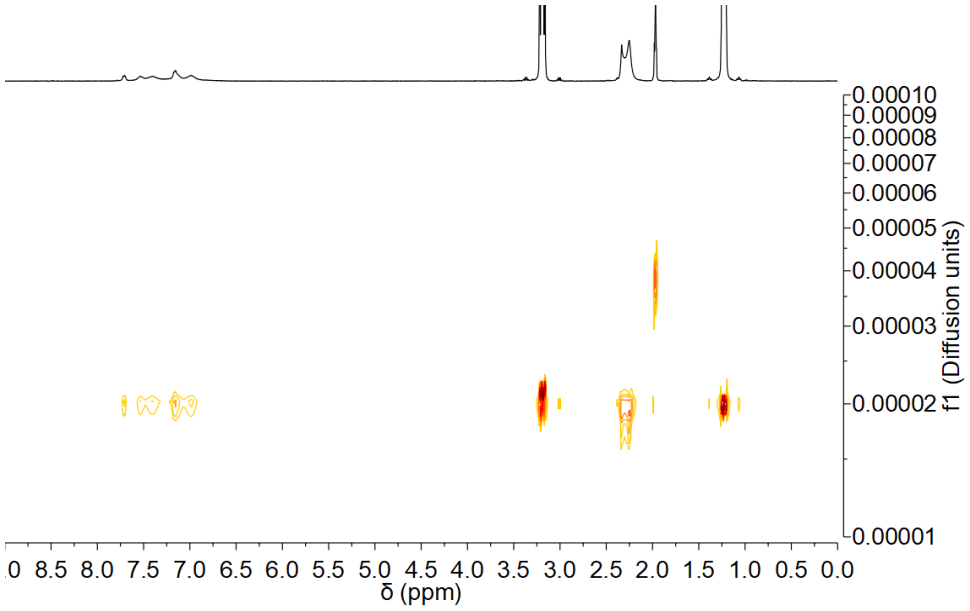

Figure S46. 2D ^{1}H DOSY plot of [Et_4N][**1^{Me}**] treated with S_8 (1 S atom equiv) and 1 equiv LiOTf in CD_3CN at 20° C.

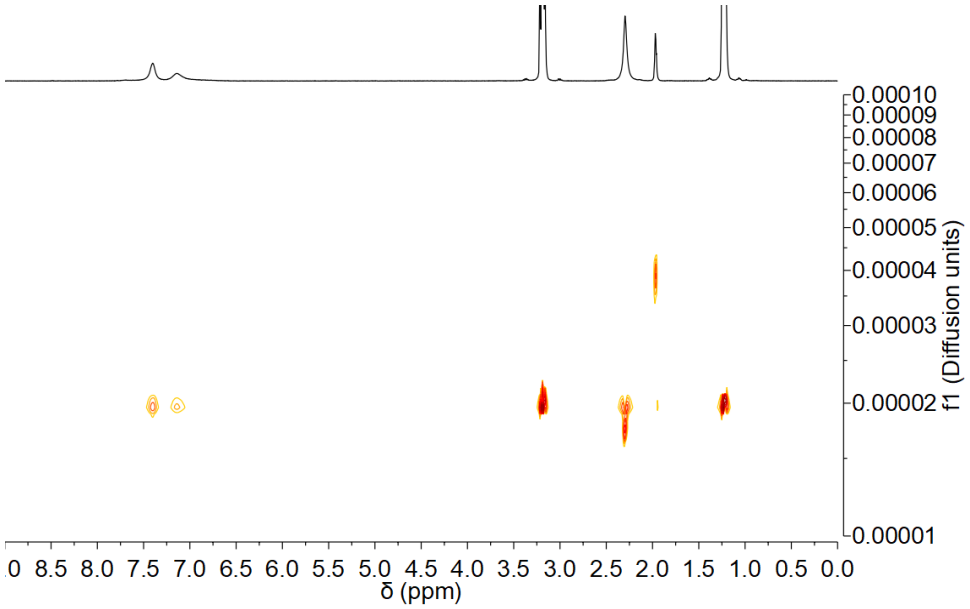

Figure S47. 2D ^{1}H DOSY plot of [Et_4N][**1^{Me}**] treated with S_8 (1 S atom equiv) and 0.25 equiv $Mg(OTf)_2$ in CD_3CN at 20° C.

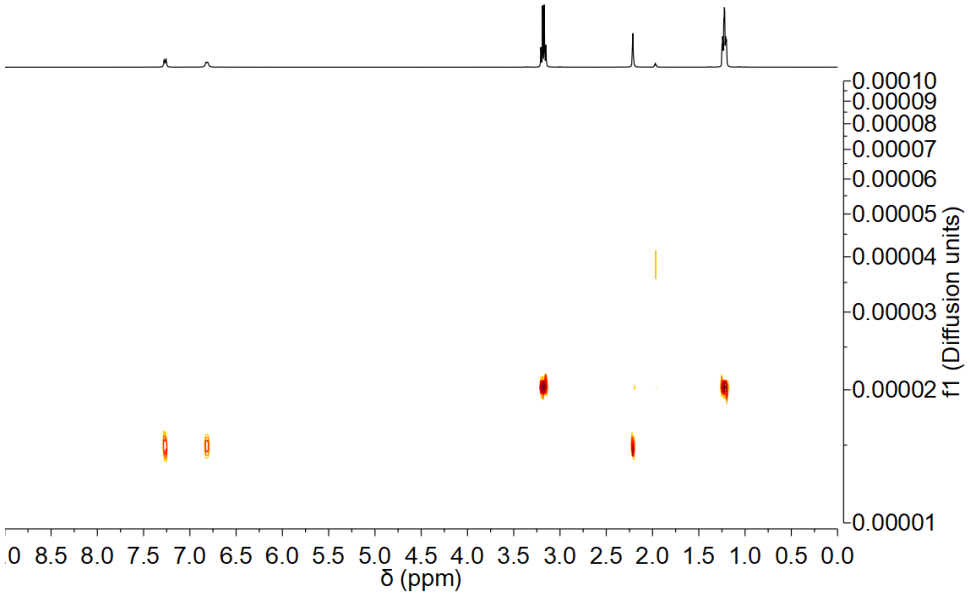

Figure S48. 2D ^{1}H DOSY plot of [Et_4N][**1^{Me}**] treated with 0.5 equiv $Mg(OTf)_2$ to form "Mg(*p*-olS)$_2$" in CD_3CN at 20° C.

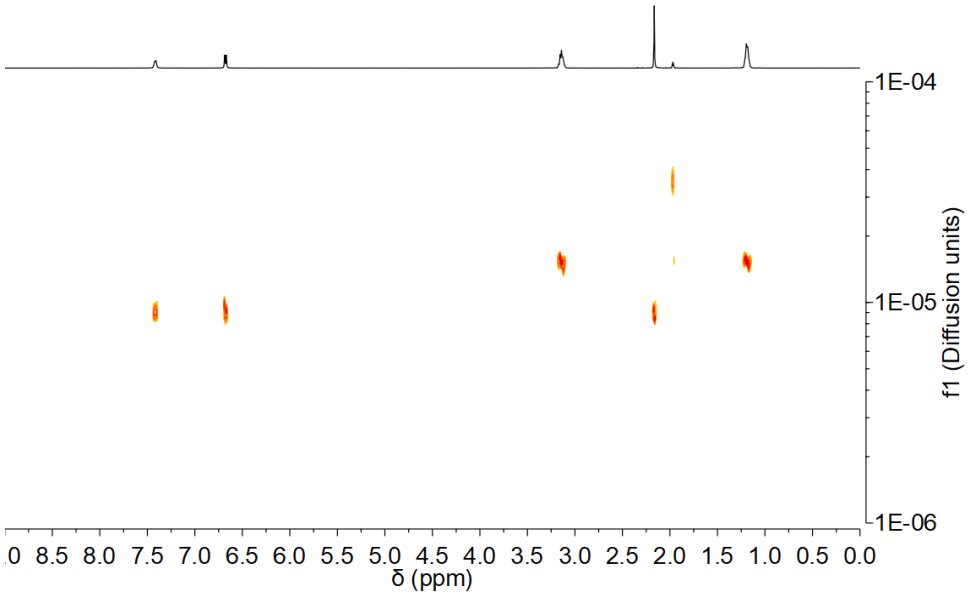

Figure S49. 2D ^{1}H DOSY plot of $[Et_4N]_2[\mathbf{4^{Me}}]$ in CD_3CN at 20° C.

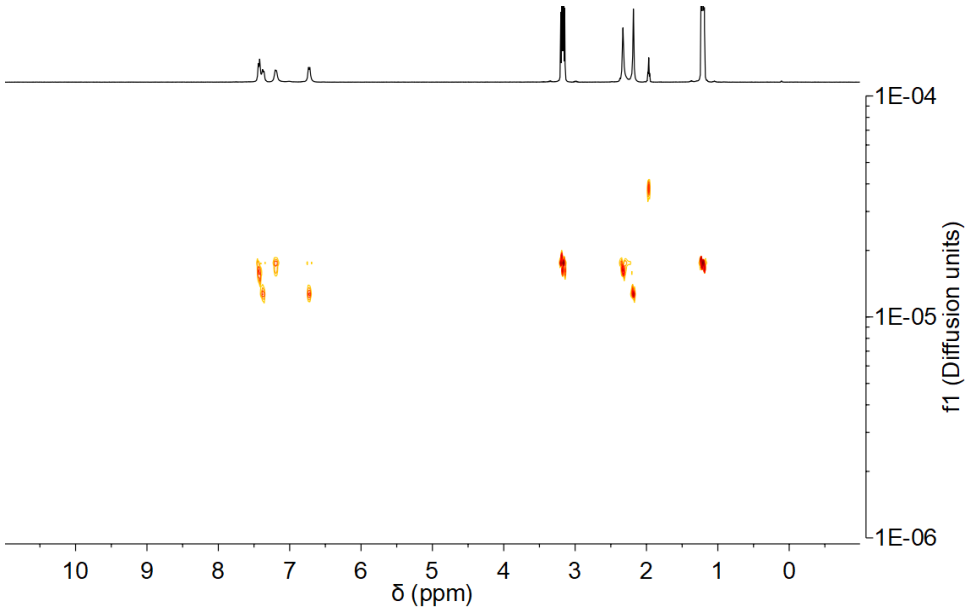

Figure S50. 2D ^{1}H DOSY plot of $[Et_4N][\mathbf{4^{Me}}]$ treated with S_8 (4 S atom equiv) to form $[\mathbf{5^{Me}}]^{2-}$ and $\mathbf{3^{Me}}$ in CD_3CN at 20° C.

Table S1. Relative diffusion coefficients and hydrodynamic radii of [1Me]− treated with S8 (1 S atom equiv), the same mixture treated with 1 equiv LiOTf, the same mixture treated with 0.25 equiv Mg(OTf)2, [1Me]− treated with 0.5 equiv Mg(OTf)2, [4Me]2−, and [5Me]2−.[3-4] Calculated molecular weight values were approximated using the Stokes-Einstein-Gierer-Wirtz model[5] with solvent parameters defined for THF-d_8 in place of CD_3CN.[3-6]

	Avg. D ($\times 10^{-9}$ m^2·s^{-1})	**Std. Error[a]**	**R_H ($\times 10^{-10}$ m)**	**MW (g·mol^{-1})**
p-tolS$^-$ + S	2.10	± 0.01	2.98	75
p-tolS$^-$ + S + LiOTf	2.02	± 0.02	3.10	81
p-tolS$^-$ + S + 0.25 Mg(OTf)$_2$	1.96	± 0.04	3.19	85
p-tolS$^-$ + 0.5 Mg(OTf)$_2$	1.49	± 0.04	4.20	143
[Zn(*p*-tolS)$_4$]$^{2-}$ + 4 S	1.26	± 0.02	4.96	199
[Zn(*p*-tolS)$_4$]$^{2-}$	0.98	± 0.03	6.36	328

ESI Mass Spectra

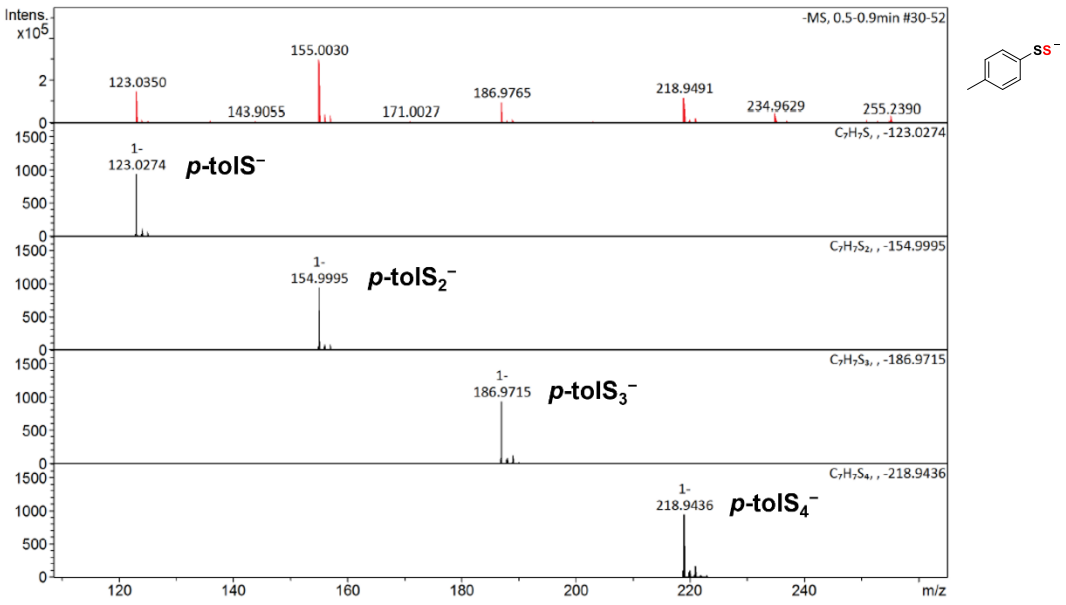

Figure S51. Negative ion mode ESI mass spectrum of a mixture of [Et$_4$N][**1^{Me}**] and 1/8 equiv S_8 in CH_3CN.

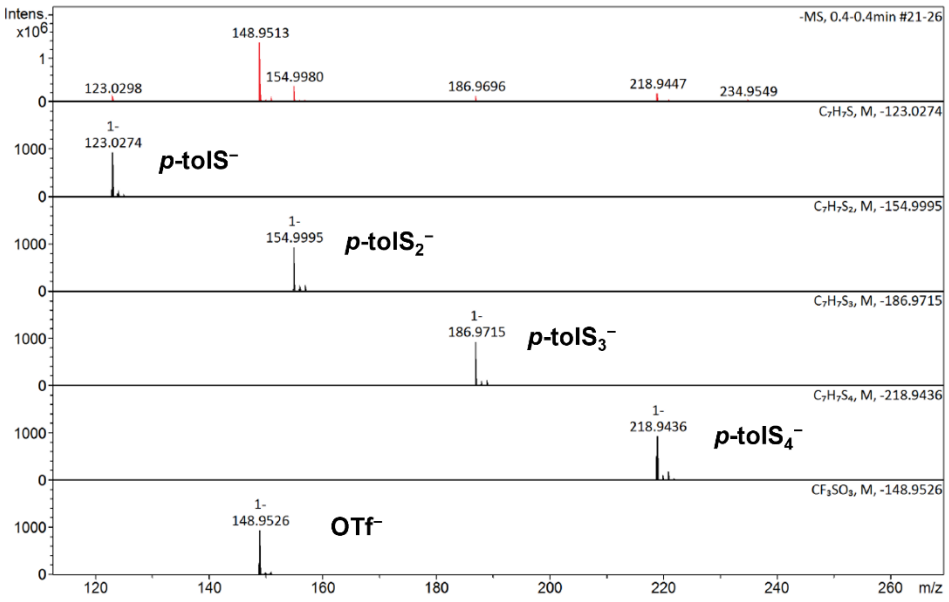

Figure S52. Negative ion mode ESI mass spectrum of a mixture of $[Et_4N][\mathbf{1^{Me}}]$ treated with 1/8 equiv S_8 and 1 equiv LiOTf in CH_3CN.

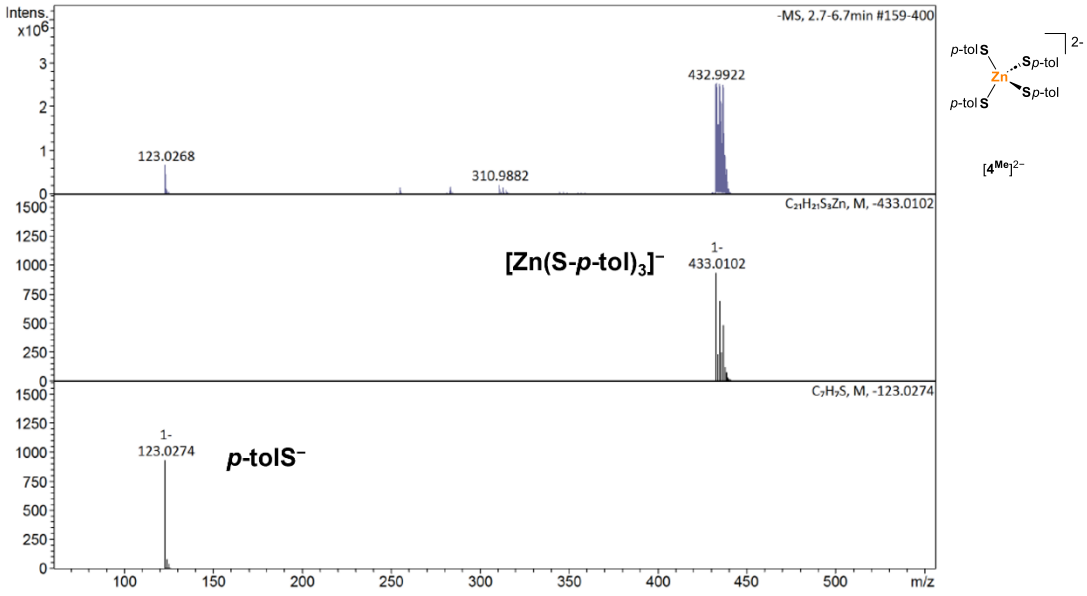

Figure S53. Negative ion mode ESI mass spectrum of $[Et_4N]_2[\mathbf{4^{Me}}]$ in CH_3CN.

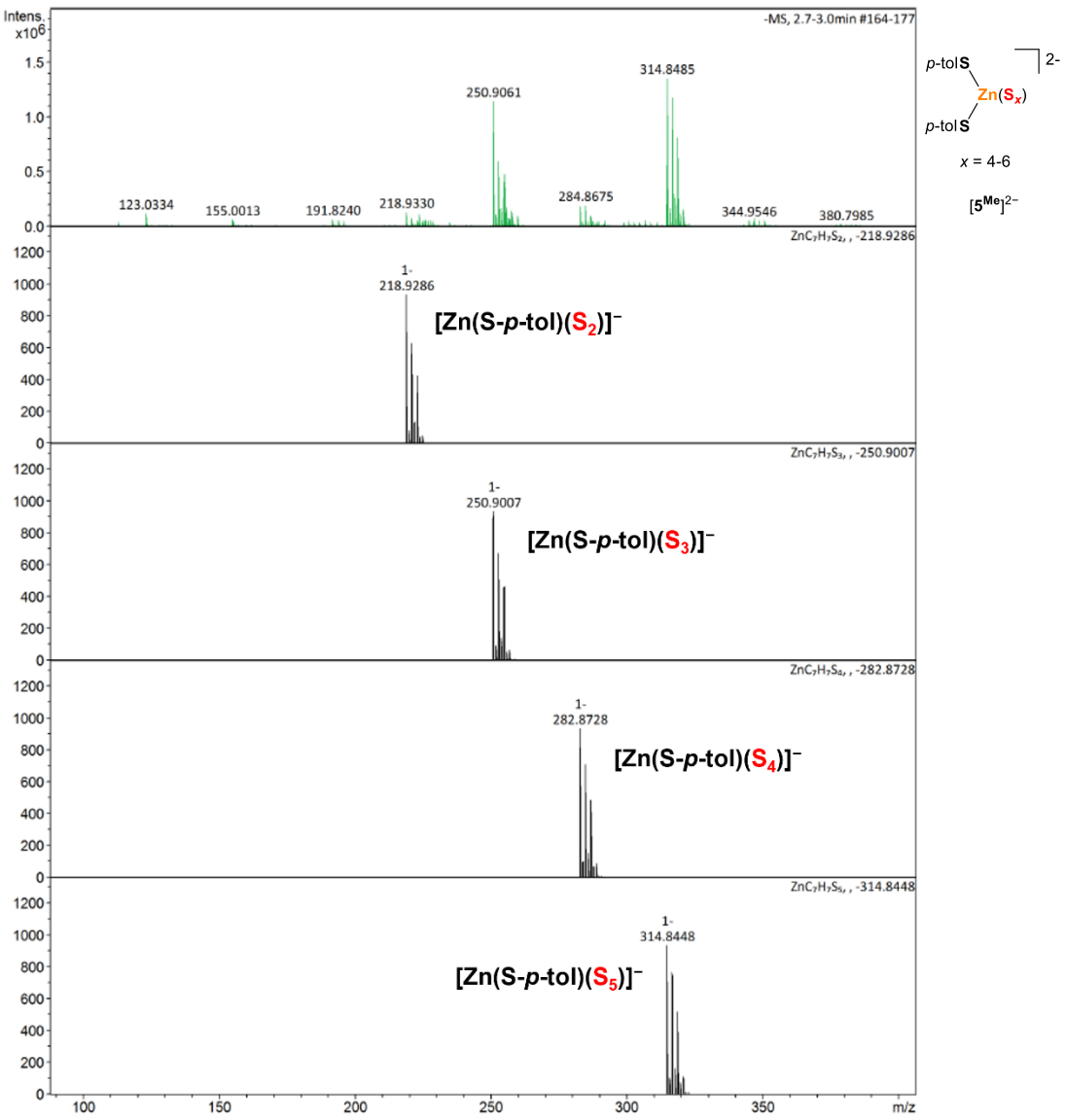

Figure S54. Negative ion mode ESI mass spectrum of $[Et_4N]_2[\mathbf{5^{Me}}]$ prepared by treating a mixture of $[Et_4N][\mathbf{1^{Me}}]$ and 1/8 equiv S_8 with 0.25 equiv $Zn(OTf)_2$ in CH_3CN.

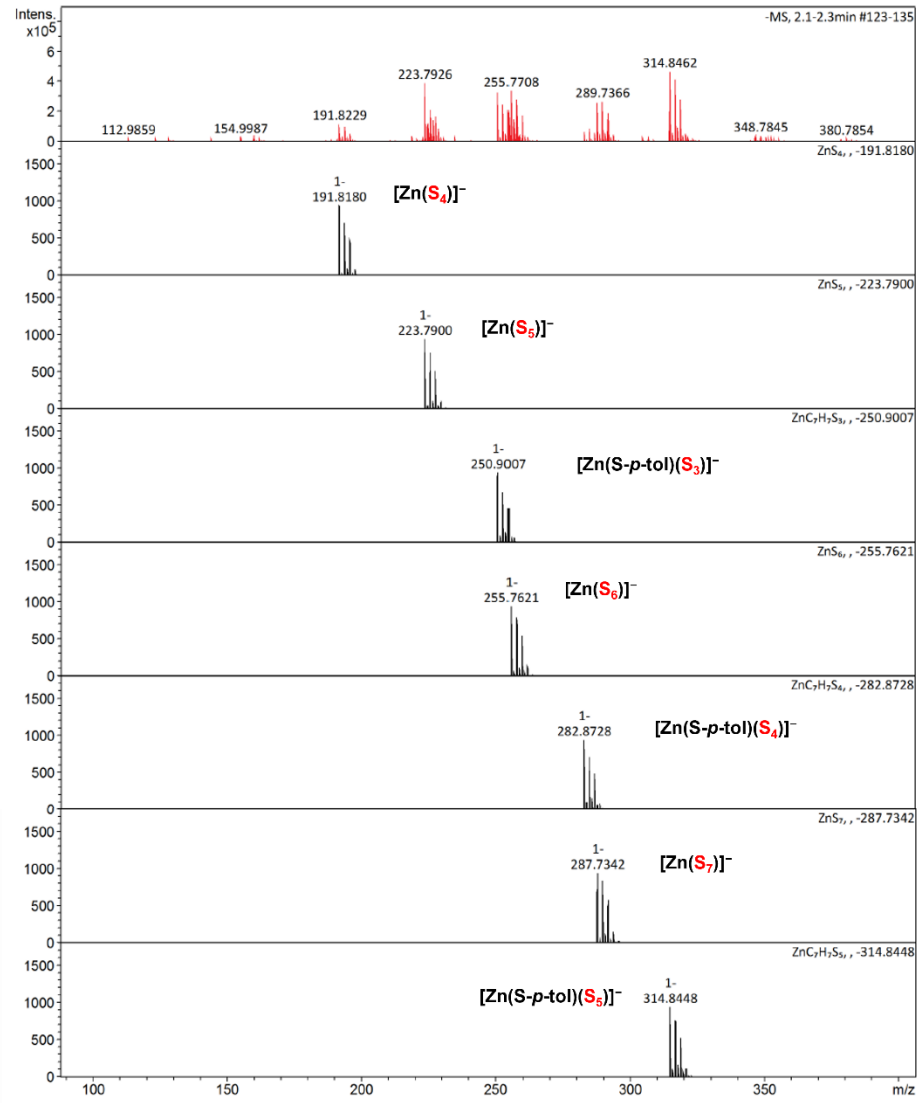

Figure S55. Negative ion mode ESI mass spectrum of $[Et_4N]_2[\mathbf{5^{Me}}]$ and $[Et_4N]_2[\mathbf{6}]$ prepared by treating a mixture of $[Et_4N]_2[\mathbf{4^{Me}}]$ with 6/8 equiv S_8 in CH_3CN.

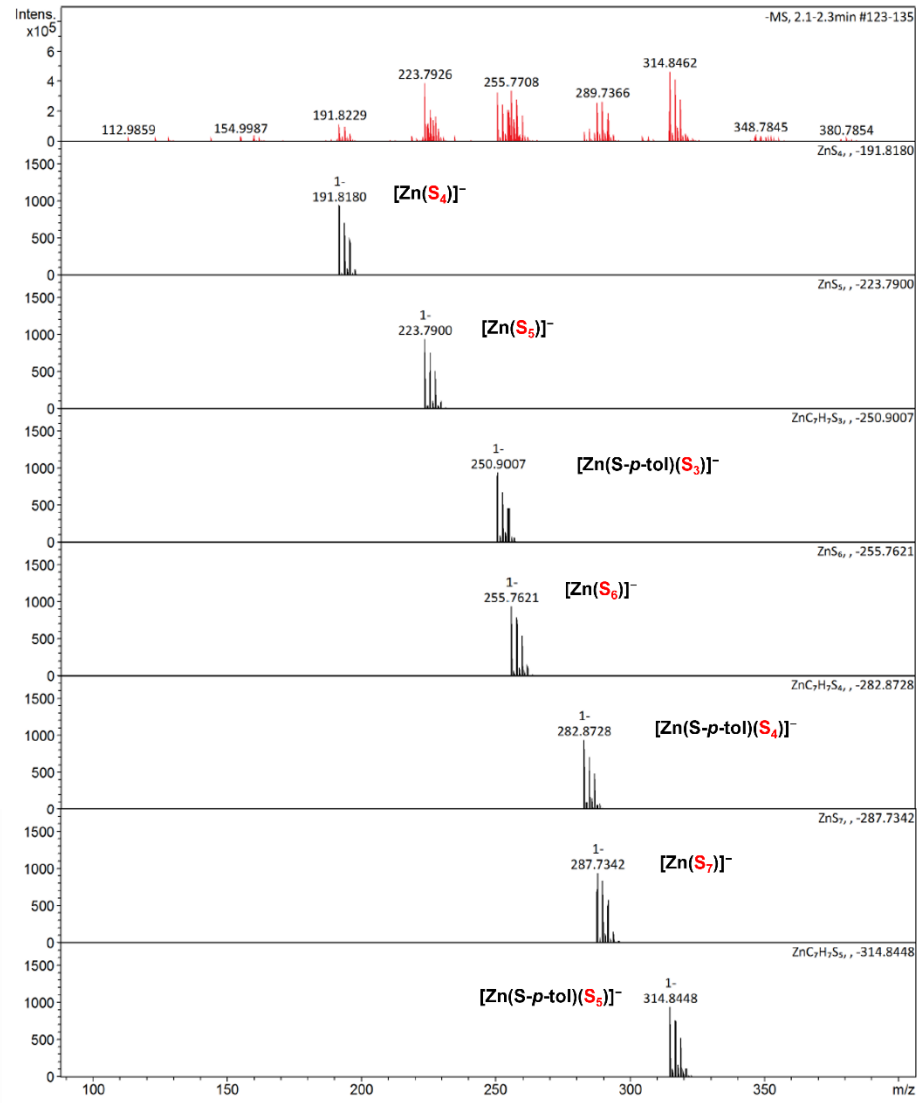

Figure S56. Negative ion mode ESI mass spectrum of $[Et_4N]_2[\mathbf{5^{Me}}]$ and $[Et_4N]_2[\mathbf{6}]$ prepared by treating a mixture of $[Et_4N]_2[\mathbf{4^{Me}}]$ with 1 equiv S_8 in CH_3CN.

Electronic Absorption Spectra

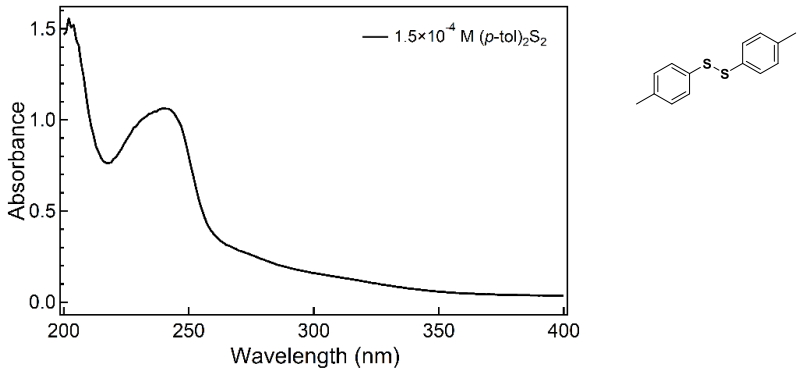

Figure S57. Electronic absorption spectrum of **3^{Me}** (1.50 ×10^{-4} M) in CH_3CN.

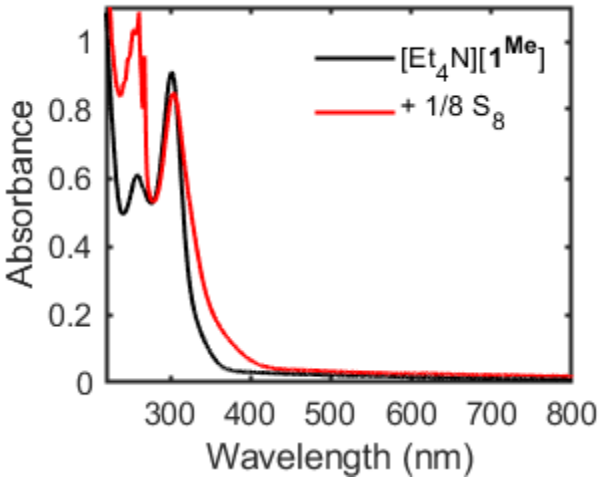

Figure S58. Electronic absorption spectra of 7.67×10^{-5} M [Et$_4$N][**1^{Me}**] (black) and [Et$_4$N][**1^{Me}**] (7.67×10^{-5} M) treated with 1/8 equiv S_8 (red) in CH_3CN.

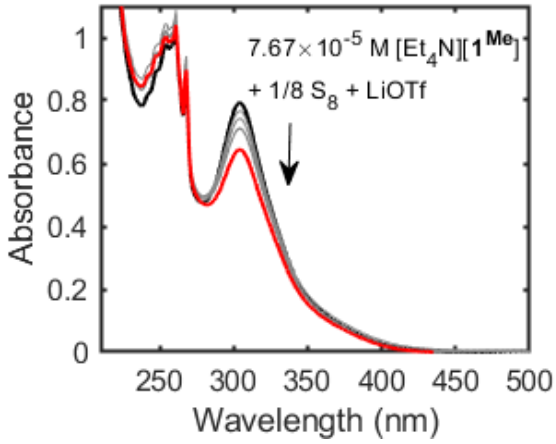

Figure S59. Electronic absorption spectra of 7.67×10^{-5} M [Et$_4$N][**1^{Me}**] (black) treated with 1/8 equiv S_8 and 1.0 equiv LiOTf (red) in CH_3CN.

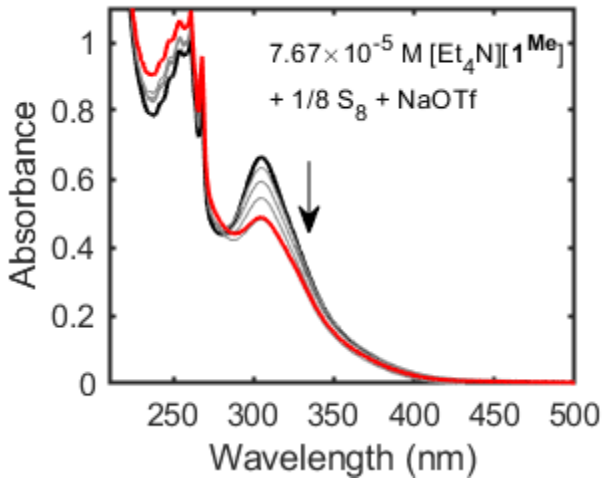

Figure S60. Electronic absorption spectra of 7.67×10^{-5} M [Et_4N][$\mathbf{1^{Me}}$] (black) treated with 1/8 equiv S_8 and 1.0 equiv NaOTf (red) in CH_3CN.

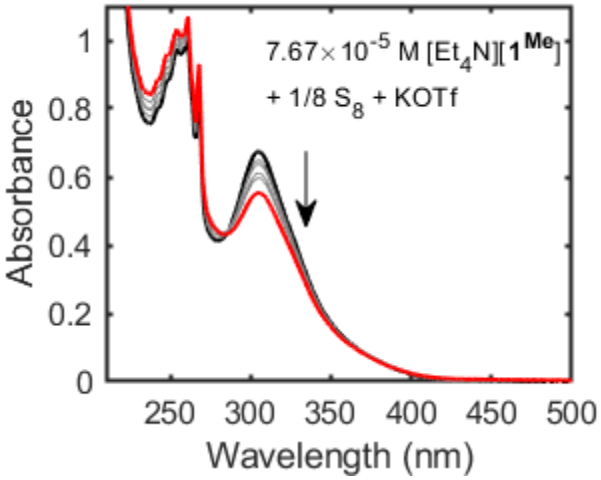

Figure S61. Electronic absorption spectra of 7.67×10^{-5} M [Et_4N][$\mathbf{1^{Me}}$] (black) treated with 1/8 equiv S_8 and 1.0 equiv KOTf (red) in CH_3CN.

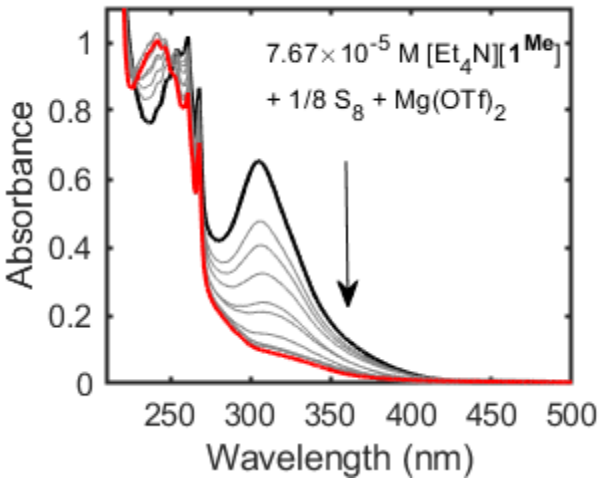

Figure S62. Electronic absorption spectra of 7.67×10^{-5} M [Et_4N][**1**^{Me}] (black) treated with 1/8 equiv S_8 and 1.0 equiv $Mg(OTf)_2$ (red) in CH_3CN.

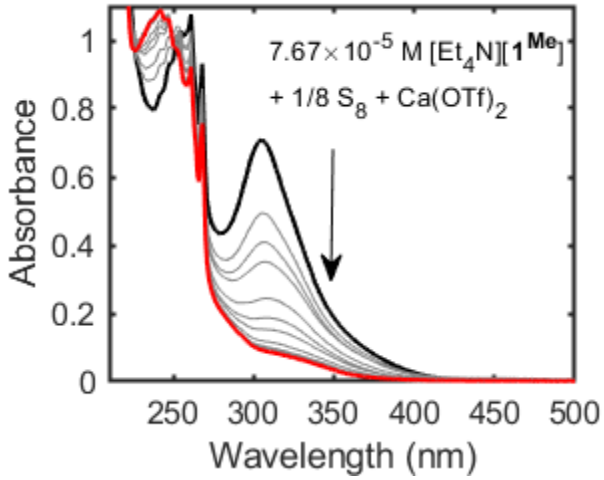

Figure S63. Electronic absorption spectra of 7.67×10^{-5} M [Et_4N][**1**^{Me}] (black) treated with 1/8 equiv S_8 and 1.0 equiv $Ca(OTf)_2$ (red) in CH_3CN.

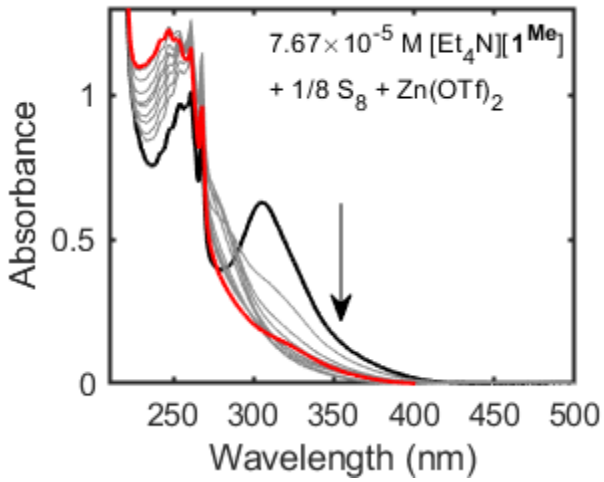

Figure S64. Electronic absorption spectra of 7.67×10^{-5} M [Et_4N][**1**^{Me}] (black) treated with 1/8 equiv S_8 and 1.0 equiv $Zn(OTf)_2$ (red) in CH_3CN.

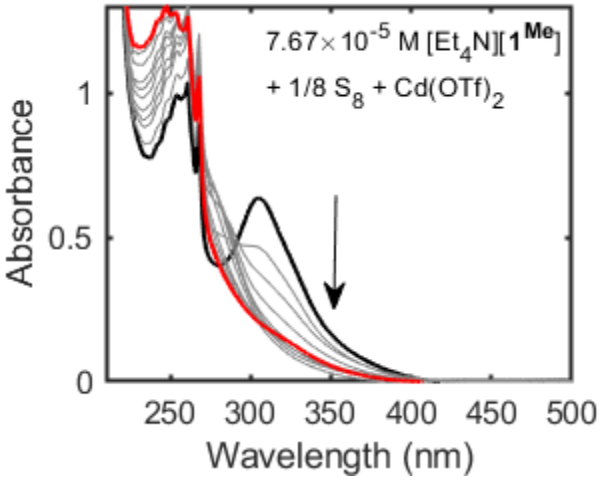

Figure S65. Electronic absorption spectra of 7.67×10^{-5} M [Et_4N][**1**^{Me}] (black) treated with 1/8 equiv S_8 and 1.0 equiv $Cd(OTf)_2$ (red) in CH_3CN.

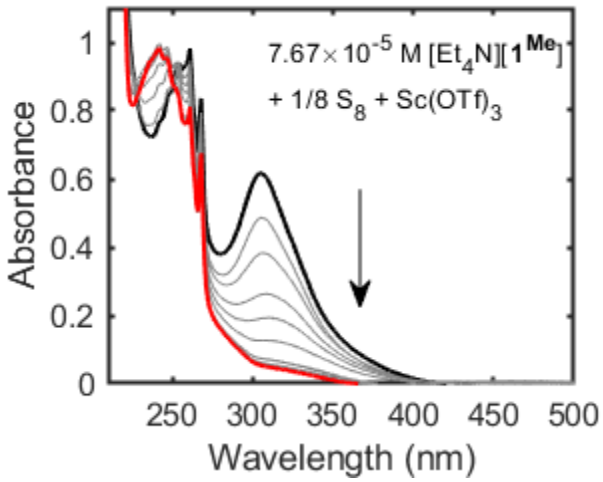

Figure S66. Electronic absorption spectra of 7.67×10^{-5} M $[Et_4N][\mathbf{1^{Me}}]$ (black) treated with 1/8 equiv S_8 and 1.0 equiv $Sc(OTf)_3$ (red) in CH_3CN.

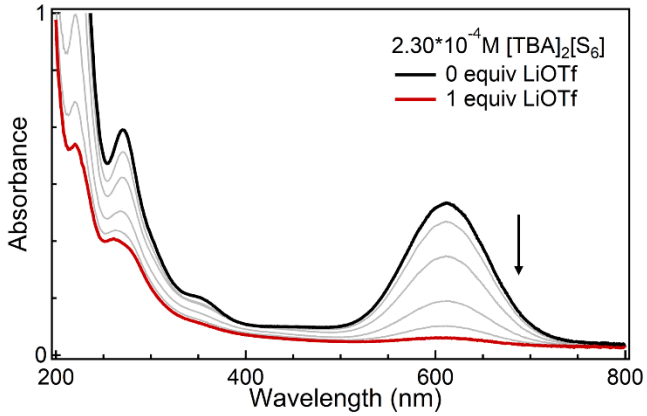

Figure S67. Electronic absorption spectra of 2.30×10^{-4} M $[TBA]_2[S_6]$ (black) treated with 1.0 equiv LiOTf (red) in CH_3CN.

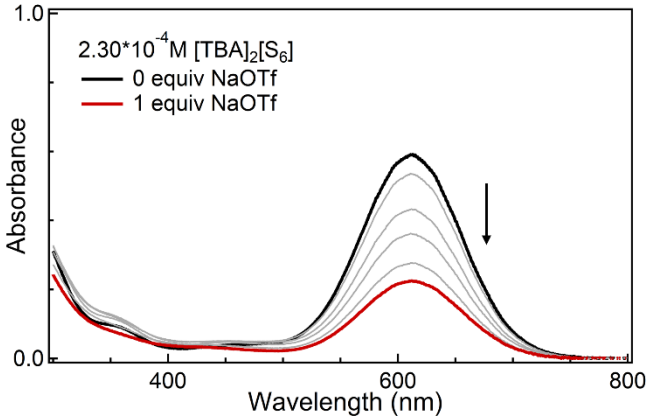

Figure S68. Electronic absorption spectra of 2.30×10^{-4} M $[TBA]_2[S_6]$ (black) treated with 1.0 equiv NaOTf (red) in CH_3CN.

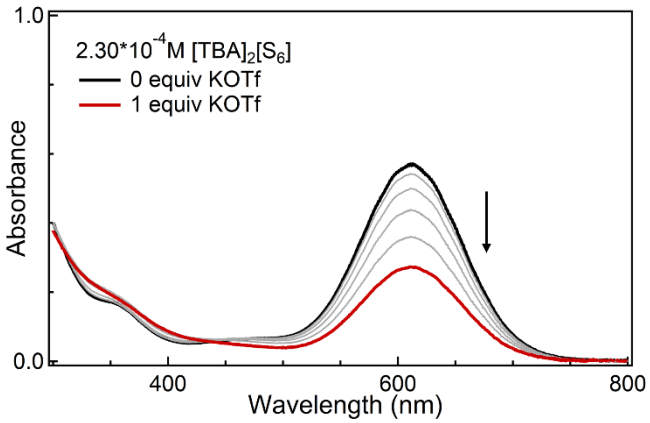

Figure S69. Electronic absorption spectra of 2.30×10^{-4} M $[TBA]_2[S_6]$ (black) treated with 1.0 equiv KOTf (red) in CH_3CN.

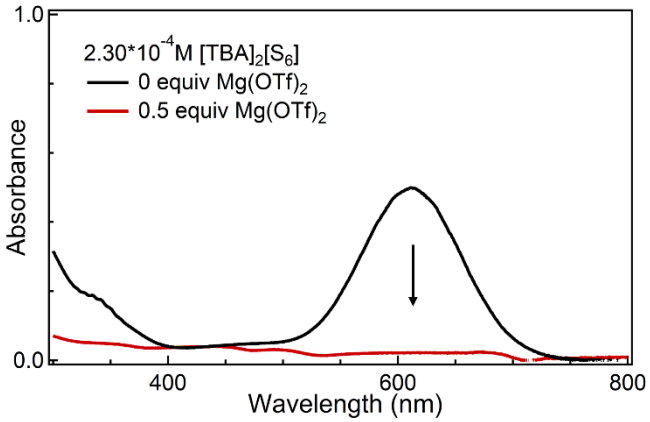

Figure S70. Electronic absorption spectra of 2.30×10^{-4} M $[TBA]_2[S_6]$ (black) treated with 0.5 equiv $Mg(OTf)_2$ (red) in CH_3CN.

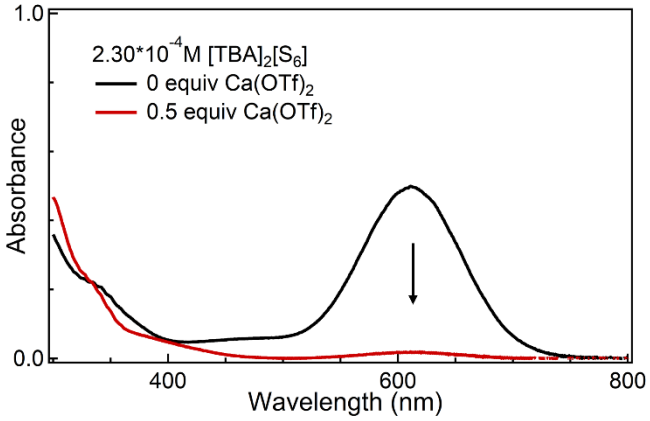

Figure S71. Electronic absorption spectra of 2.30×10^{-4} M $[TBA]_2[S_6]$ (black) treated with 0.5 equiv $Ca(OTf)_2$ (red) in CH_3CN.

Cyclic Voltammograms

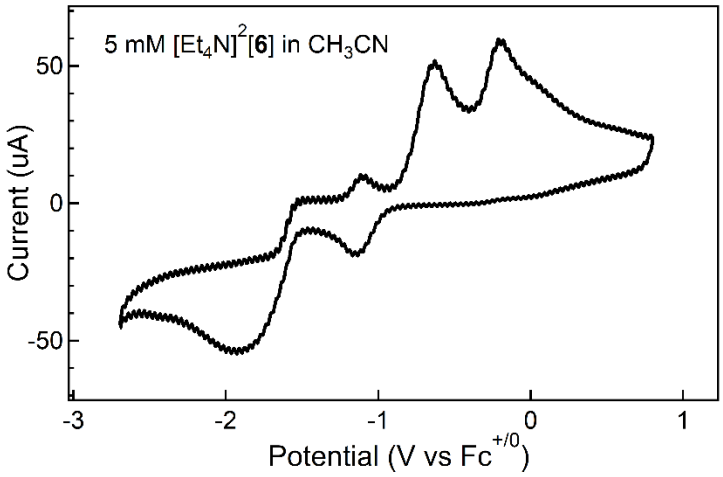

Figure S72. Cyclic voltammogram of $[Et_4N]_2$[**6**] (5mM) and 0.1 M $TBAPF_6$ in CH_3CN.

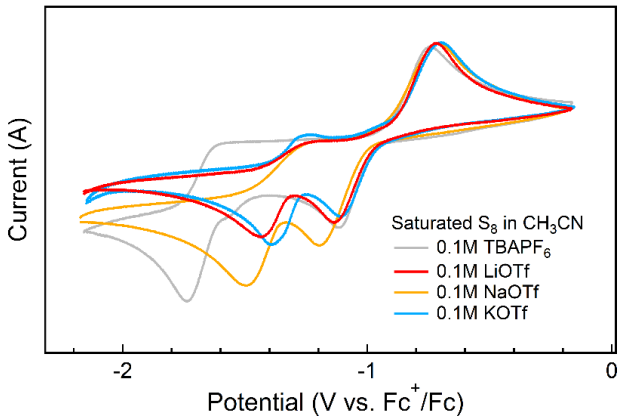

Figure S73. Cyclic voltammograms of solutions of saturated S_8 and 0.1 M Li^+, Na^+, and K^+ triflate salts in CH_3CN.

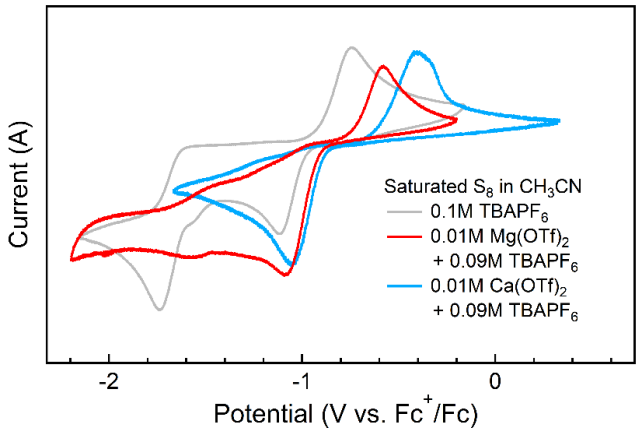

Figure S74. Cyclic voltammograms of solutions of saturated S_8, 0.09 M $TBAPF_6$, and 0.01 M Mg^{2+} and Ca^{2+} triflate salts in CH_3CN.

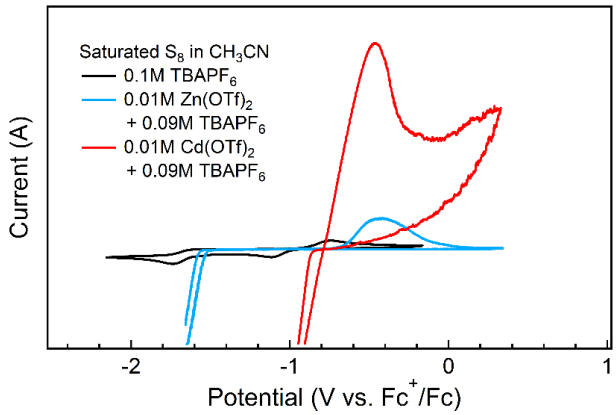

Figure S75. Cyclic voltammograms of solutions of saturated S_8, 0.09 M $TBAPF_6$, and 0.01 M Zn^{2+} and Cd^{2+} triflate salts in CH_3CN.

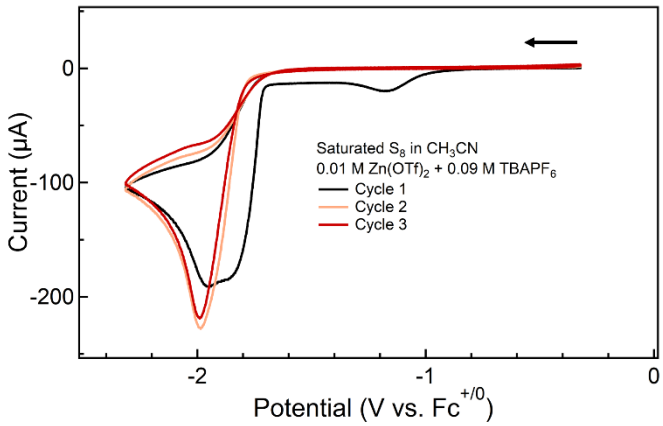

Figure S76. Cyclic voltammograms of a solution of saturated S_8, 0.09 M $TBAPF_6$, and 0.01 M $Zn(OTf)_2$ in CH_3CN demonstrating disappearance of initial S_8 reduction after the first cycle.

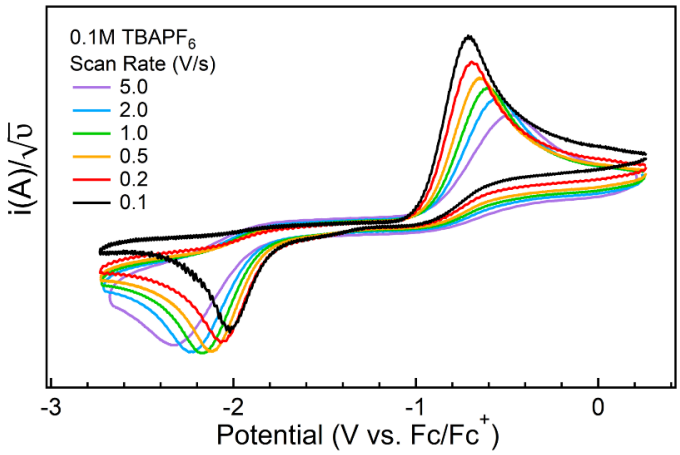

Figure S77. Cyclic voltammograms at varying scan rates of 5mM $[Et_4N][\mathbf{1^{Me}}]$ and 0.1 M $TBAPF_6$ in CH_3CN.

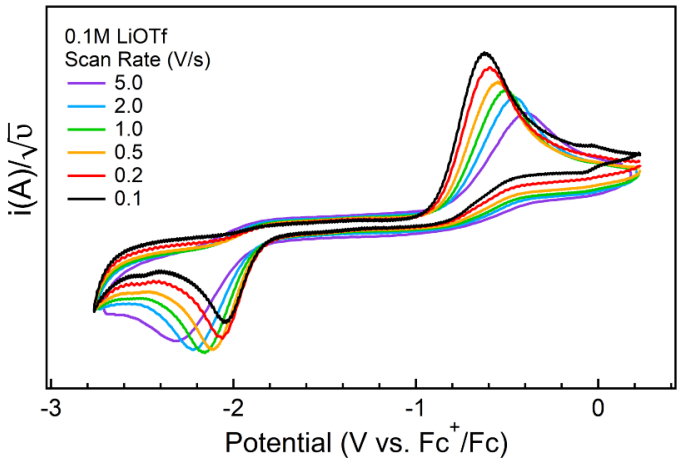

Figure S78. Cyclic voltammograms at varying scan rates of 5mM [Et_4N][**1**^{Me}] and 0.1 M LiOTf in CH_3CN.

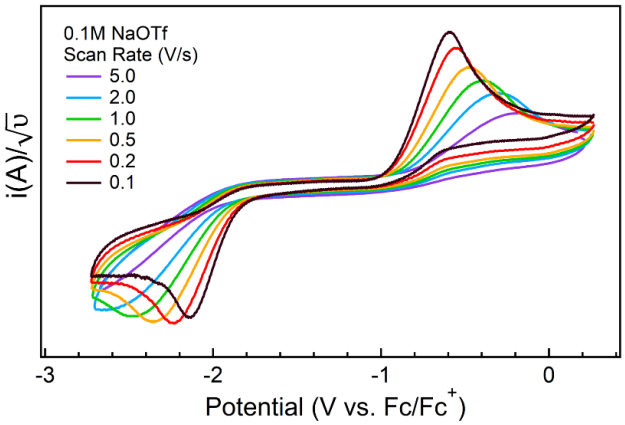

Figure S79. Cyclic voltammograms at varying scan rates of 5mM [Et_4N][**1**^{Me}] and 0.1 M NaOTf in CH_3CN.

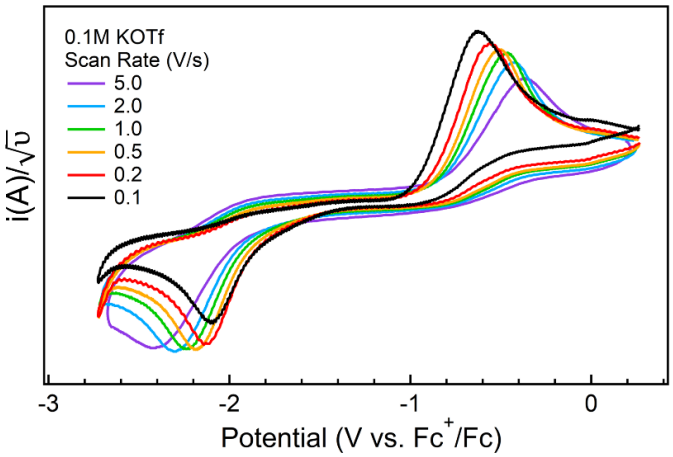

Figure S80. Cyclic voltammograms at varying scan rates of 5mM [Et_4N][**1**^{Me}] and 0.1 M KOTf in CH_3CN.

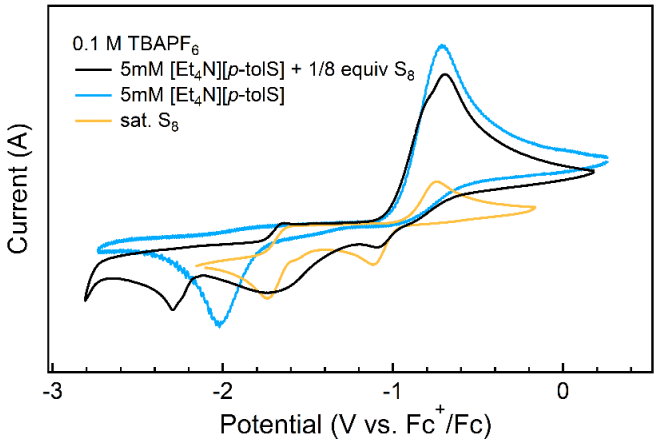

Figure S81. Cyclic voltammogram of 5mM [Et_4N][**1**^{Me}] treated with 1/8 equiv S_8 in 0.1 M $TBAPF_6$ in CH_3CN compared against those of [Et_4N][**1**^{Me}] and S_8.

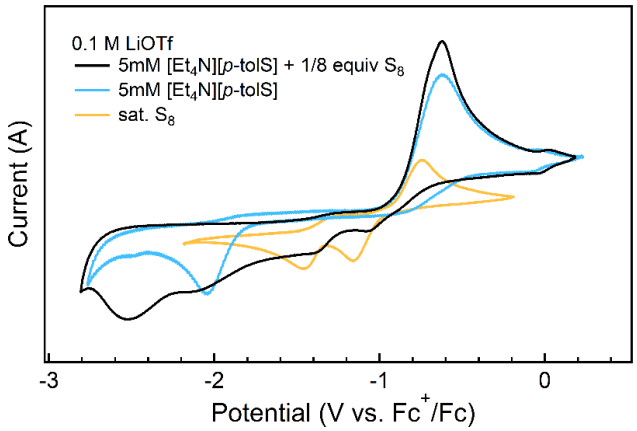

Figure S82. Cyclic voltammogram of 5mM [Et_4N][**1**^{Me}] treated with 1/8 equiv S_8 in 0.1 M LiOTf in CH_3CN compared against those of [Et_4N][**1**^{Me}] and S_8.

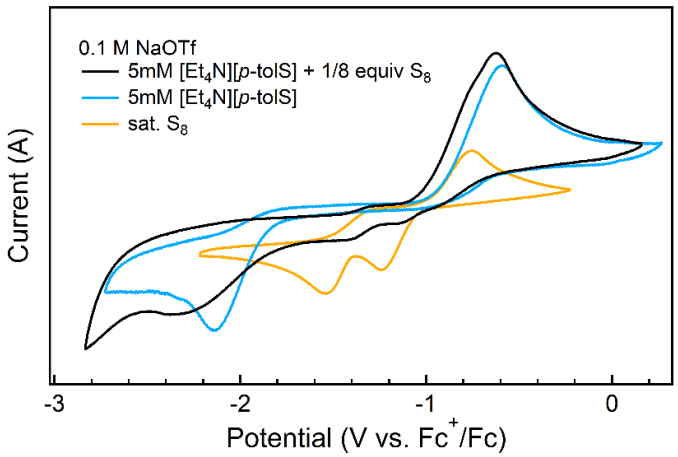

Figure S83. Cyclic voltammogram of 5mM [Et_4N][**1**^{Me}] treated with 1/8 equiv S_8 in 0.1 M NaOTf in CH_3CN compared against those of [Et_4N][**1**^{Me}] and S_8.

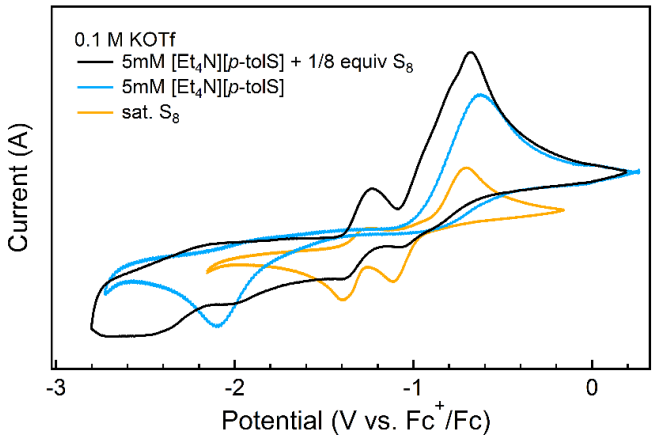

Figure S84. Cyclic voltammogram of 5mM [Et$_4$N][**1^{Me}**] treated with 1/8 equiv S_8 in 0.1 M KOTf in CH_3CN compared against those of [Et$_4$N][**1^{Me}**] and S_8.

Powder X-ray Diffraction

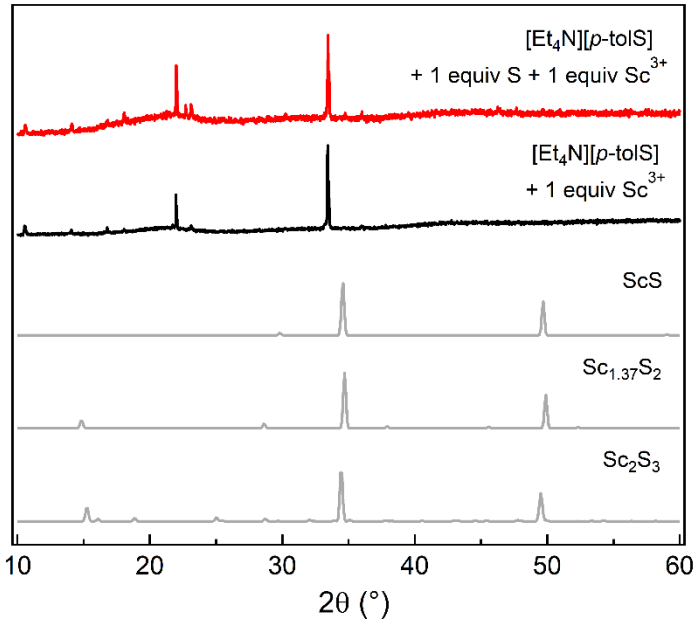

Figure S85. PXRD of [Et$_4$N][**1^{Me}**] treated with S_8 (1 equiv S) and $Sc(OTf)_3$, attributed to scandium thiolate species and no matches to any patterns corresponding to structurally characterized scandium sulfide compounds reported in the ICSD (bottom half).

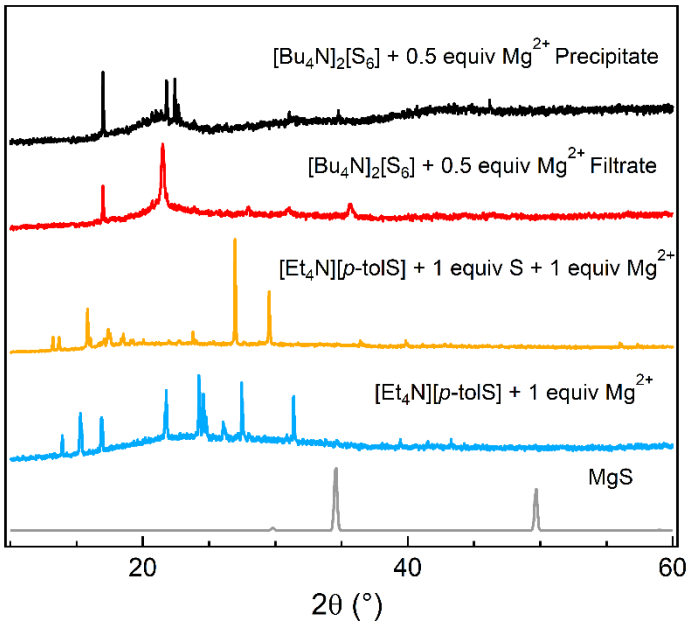

Figure S86. PXRD of [*n*-Bu$_4$N]$_2$[S$_6$] and [Et$_4$N][**1^{Me}**] treated with S$_8$ (1 equiv S) and Mg(OTf)$_2$, attributed to magnesium thiolate and magnesium sulfide species with no match to structurally characterized MgS reported in the ICSD (bottom).

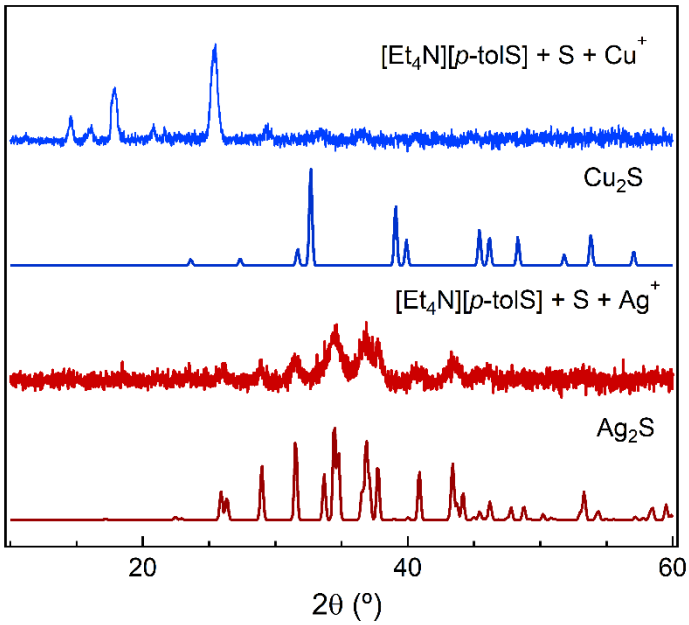

Figure S87. PXRD of [Et$_4$N[**1^{Me}**] treated with S$_8$ (1 equiv S) and (CH$_3$CN)$_4$CuPF$_6$ or AgOTf (1 equiv) with comparison to literature pattern for Cu$_2$S and Ag$_2$S obtained from ICSD. The pattern obtained with Cu$^+$ does not fit any of those corresponding to structurally characterized compounds reported in the ICSD.

Crystallographic Details. CCDC 2332488 contains the supplementary crystallographic data for this paper. These data can be obtained free of charge from The Cambridge Crystallographic Data Centre via www.ccdc.cam.ac.uk/data_request.cif.

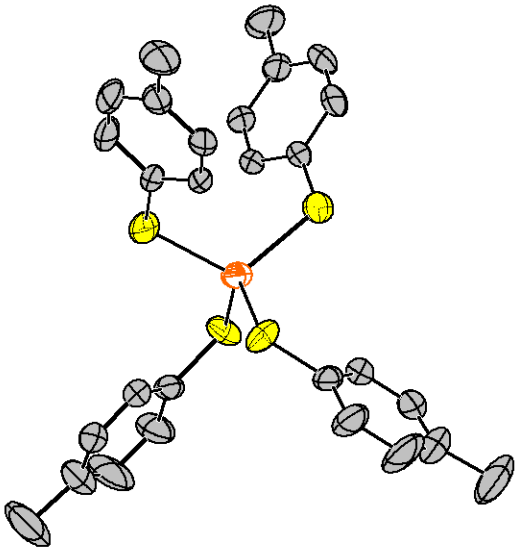

Figure S88. Solid-state structure of $[Et_4N]_2[\mathbf{4^{Me}}]$ drawn as 50% thermal ellipsoids. Hydrogen atoms and countercations omitted for clarity.

Refinement details for $[Et_4N]_2[\mathbf{4^{Me}}]$. Crystals of $[Et_4N]_2[\mathbf{4^{Me}}]$ were grown from slow cooling of a saturated solution in CH_3CN at −30°C. Crystals were mounted on a MiTeGen loop using Paratone oil, then placed on the diffractometer under a cold nitrogen stream. An arbitrary sphere of data was collected on a colorless prism, having approximate dimensions 0.236 × 0.262 × 0.578 mm, on a Bruker APEX-II CCD diffractometer using a combination of ω- and φ-scans of 0.5°.[7] Data were corrected for absorption and polarization effects and analyzed for space group determination.[8] The structure was solved by dual-space methods and expanded routinely.[9] The model was refined by full-matrix least-squares analysis of F^2 against all reflections.[10] The Et_4N cations were found to be disordered across two independent inversion centers. Each was modeled with half occupancy atoms that were refined independent from all symmetry (PART −1). Non-hydrogen atoms were refined with anisotropic displacement parameters with hydrogen atoms riding on the atom to which they are bonded (U_{iso}(H) = 1.5U_{eq}(C) for methyl, 1.2U_{eq}(C) for all others). No additional restraints or constraints were applied.

Table S2. Crystal and refinement data.

Compound	**$[Et_4N]_2[4^{Me}]$**
Empirical formula	$C_{44}H_{68}N_2S_4Zn$
Formula weight	818.63
Temperature	120.0 K
Wavelength	0.71073 Å
Crystal system	Tetragonal
Space group	$P4_32_12$
Unit cell dimensions	a = 15.6496(8) Å b = 15.6496(8) Å c = 18.1435(13) Å α = 90° β = 90° γ = 90°
Volume	4443.5(6) $Å^3$
Z	4
Density (calculated)	1.224 $g \cdot cm^3$
Absorption coefficient (μ)	0.772 mm^{-1}
F(000)	1760
Crystal color, habit	Colorless prism
Crystal size	0.236 × 0.262 × 0.578 mm
θ range for data collection	1.718 to 27.499
Index ranges	$-20 \leq h \leq 20$, $-20 \leq k \leq 20$, $-22 \leq l \leq 23$
Reflections collected	64360
Independent reflections	5113 [R_{int} = 0.0954]
Completeness to θ = 25.242°	100%
Absorption correction	Semi-empirical from equivalents
Max. and min. transmission	0.6632 and 0.7868
Refinement method	Full-matrix least-squares on F^2
Data / restraints / parameters	5113 / 0 /322
Goodness-of-fit on F^2	1.076
Final R indices [$I \geq 4\sigma(F_0)$]	R_1 = 0.0445 wR_2 = 0.0970
R indices (all data)	R_1 = 0.0513 wR_2 = 0.1018
Extinction coefficient	n/a
Largest diff. peak / hole	0.392 / −0.367

Computational Details

Density functional theory (DFT) calculations were performed using the Gaussian 16 program.[11]

The electronic absorption spectra of [**1**$^{\mathbf{H}}$]$^{-}$ and [**2**$^{\mathbf{H}}$]$^{-}$ were calculated by TD-DFT (20 states) based on optimized geometries calculated using the B3LYP functional with the 6-311 +G(2d,p) basis set using PCM solvation with acetonitrile.

Table S3. Optimized coordinates for [**1**$^{\mathbf{H}}$]$^{-}$ with CH_3CN solvation (Å).

Number	Atom	x	y	z
1	S	2.3489	0.0000	0.0000
2	C	0.5759	0.0000	0.0000
3	C	-0.1645	-1.1992	0.0000
4	H	0.3680	-2.1436	0.0001
5	C	-1.5556	-1.1986	0.0000
6	H	-2.0873	-2.1445	0.0001
7	C	-2.2677	0.0000	0.0000
8	H	-3.3512	0.0000	-0.0003
9	C	-1.5555	1.1987	0.0000
10	H	-2.0873	2.1445	0.0000
11	C	-0.1645	1.1992	0.0000
12	H	0.3681	2.1435	0.0001

Table S4. Optimized coordinates for [**2**$^{\mathbf{H}}$]$^{-}$ with CH_3CN solvation (Å).

Number	Atom	x	y	z
1	S	-2.75086	0.645699	0.000188
2	S	-1.42445	-0.96207	-0.00022
3	C	0.229056	-0.33388	-3.8E-05
4	C	0.533871	1.033857	-0.00016
5	H	-0.29019	1.735495	-0.0002
6	C	1.857661	1.459705	-9.3E-05
7	H	2.069632	2.522943	-4.9E-05
8	C	2.909596	0.545639	0.000049
9	H	3.937702	0.884223	-9.6E-05
10	C	2.609914	-0.82007	0.000107
11	H	3.411065	-1.55023	0.000352
12	C	1.293413	-1.25436	0.000145
13	H	1.075616	-2.31579	0.00043

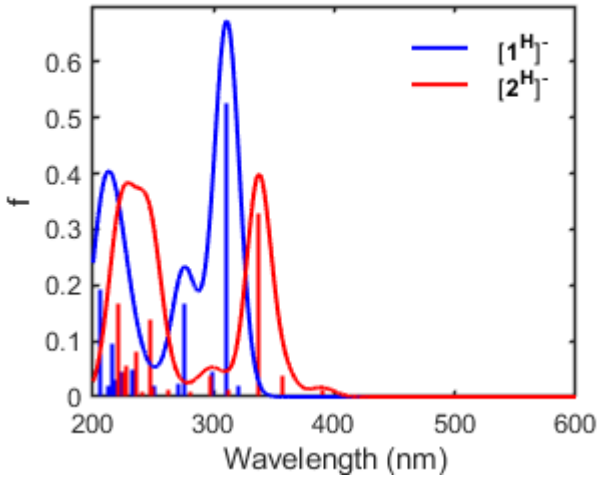

Figure S89. Simulated electronic absorption spectra for $[\mathbf{1^H}]^-$ (blue) and $[\mathbf{2^H}]^-$ (red).

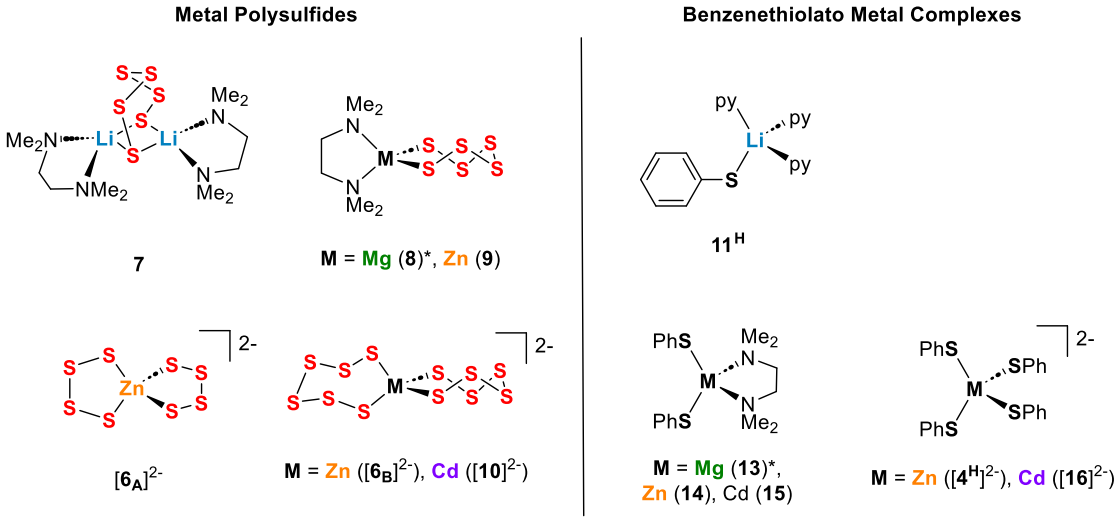

Figure S90. Drawings of complexes optimized using DFT.

Optimized geometries of metal complexes shown in Fig. S73 were calculated using the B3LYP functional basis sets as described as in Table S5. The interaction energies between polysulfide or benzenethiolate anions and metal fragments were calculated using the counterpoise (BSSE) correction.[12-13] Ionic energetic contributions (E_{ionic}) were calculated using Natural Population Analysis (NPA) and subtracted from the interaction energy to yield the covalent energetic contributions (E_{cov}).

Table S5. Complexes and fragments calculated, with basis sets, interaction energies, BSSE correction, E_{ionic}, and E_{cov}. All energies reported in kcal/mol unless otherwise indicated.

Compound	M^{n+}	Fragment	Basis Set	BSSE (a.u.)	$E_{interactions}$	E_{ionic}	E_{cov}
11^{H}*	Li^{+}	PhS^{-}	6-311 +G(3df)	0.001776772700	-90.7051	-82.83	-7.875110931
13*	Mg^{2+}	PhS^{-}	6-311 +G(3df)	0.003993009237	-135.24	-118.4093	-16.83054106
14	Zn^{2+}	PhS^{-}	6-311 +G(3df)	0.002109729748	-139.384	-42.921	-96.46273478
[$\mathbf{4^{H}}$]$^{2-}$	Zn^{2+}	PhS^{-}	6-31 +G(d,p)	0.002144696819	16.33029	34.44975	-18.11946123
[**16**]$^{2-}$	Cd^{2+}	PhS^{-}	C,H,S: 6-311 +G(3df) Cd: LANL2DZ	0.001921188647	18.42759	20.9585	-2.530905878
7	Li^{+}	S_6^{2-}	6-31 G(d,p)	0.018445172823	-375.859	-295.5525	-80.30639144
8*	Mg^{2+}	S_6^{2-}	6-311 +G(3df)	0.003993009237	-437.726	-329.563	-108.1634803
9	Zn^{2+}	S_6^{2-}	6-311 +G(3df)	0.003153131171	-446.629	-134.4733	-312.1553545
[$\mathbf{6_A}$]$^{2-}$	Zn^{2+}	S_4^{2-}	6-311 +G(3df)	0.002828392891	-116.788	17.50725	-134.2947962
[$\mathbf{6_B}$]$^{2-}$	Zn^{2+}	S_6^{2-}	6-311 +G(3df)	0.003384120439	-99.5436	17.57	-117.1136066
[**10**]$^{2-}$	Cd^{2+}	S_6^{2-}	S: 6-311 +G(3df) Cd: LANL2DZ	0.002890740856	-102.65	-21.39775	-81.25232148

(*) indicates compounds that have not been structurally characterized.

Table S6. Optimized coordinates (Å) and NPA charges for complex **11^{H}**.

Number	Atom	q_{NPA}	x	y	z
1	Li	0.81085	-0.60973	-0.00245	-0.05076
2	N	-0.53192	-0.263	-1.49099	1.401699
3	C	0.06183	-1.05513	-1.8358	2.420973
4	C	-0.24384	-0.75875	-2.86505	3.301883
5	C	-0.15468	0.421096	-3.57476	3.116155
6	C	-0.23139	1.249015	-3.22692	2.059224
7	C	0.07499	0.869864	-2.1819	1.225637
8	N	-0.5298	-2.45746	-0.43518	-0.97787
9	C	0.06321	-3.65855	0.023255	-0.61466
10	C	-0.24219	-4.82976	-0.29579	-1.28619
11	C	-0.15557	-4.75135	-1.1302	-2.3937
12	C	-0.23292	-3.50757	-1.60568	-2.78312
13	C	0.07425	-2.38836	-1.23389	-2.04941

14	N	-0.53448	-0.73652	1.939489	0.780478
15	C	0.07073	-0.27156	2.884006	-0.04697
16	C	-0.23199	-0.2598	4.23274	0.285175
17	C	-0.15436	-0.74399	4.621512	1.525732
18	C	-0.24257	-1.22209	3.646044	2.39148
19	C	0.06082	-1.19717	2.323292	1.974624
27	H	0.18018	-1.97291	-1.26601	2.533153
28	H	0.21318	-1.43903	-3.10306	4.110482
29	H	0.21038	0.687757	-4.38584	3.78434
30	H	0.21947	2.17833	-3.75115	1.874398
31	H	0.22893	1.480477	-1.88132	0.381526
32	H	0.18464	-3.68136	0.680361	0.249349
33	H	0.2135	-5.7775	0.105414	-0.94841
34	H	0.21043	-5.64463	-1.40051	-2.94539
35	H	0.21746	-3.39631	-2.25186	-3.64505
36	H	0.22299	-1.39431	-1.56978	-2.32718
37	H	0.22998	0.11466	2.523997	-0.99628
38	H	0.21842	0.130084	4.95699	-0.41931
39	H	0.21078	-0.74496	5.6658	1.817044
40	H	0.21384	-1.60344	3.900678	3.372788
41	H	0.18218	-1.55589	1.534866	2.629542
20	S	-0.55918	0.927182	-0.09617	-1.88197
21	C	-0.16622	2.618865	0.000237	-1.40568
22	C	-0.25292	3.037893	0.535865	-0.17402
23	C	-0.20531	4.382353	0.602078	0.173073
24	C	-0.25204	5.363198	0.13754	-0.69639
25	C	-0.20229	4.97045	-0.39418	-1.92279
26	C	-0.23035	3.629115	-0.46179	-2.27008
42	H	0.19238	2.292079	0.912938	0.517637
43	H	0.19363	4.664048	1.02474	1.13291
44	H	0.19597	6.411951	0.19059	-0.42672
45	H	0.1957	5.719187	-0.76057	-2.61845
46	H	0.20331	3.338285	-0.87716	-3.22842

Table S7. Optimized coordinates (Å) and NPA charges for complex **13**.

Number	Atom	q_{NPA}	x	y	z
2	S	-0.6057	1.514999	-0.17011	1.504245
3	N	-0.67221	-0.91041	2.392888	1.134118
4	N	-0.67226	1.031154	2.320227	-1.15218
5	C	-0.35317	-2.36862	2.220898	1.26556
6	H	0.21665	-2.80392	2.022836	0.287051
7	H	0.17562	-2.83183	3.115104	1.705144
8	H	0.20823	-2.57471	1.366527	1.910175
9	C	-0.35384	-0.31262	2.546574	2.472115
10	H	0.20581	0.767975	2.656044	2.401565
11	H	0.21058	-0.51657	1.654702	3.063471
12	H	0.17718	-0.73254	3.421692	2.987615
13	C	-0.18594	-0.60478	3.554055	0.272321
14	H	0.20804	-1.33181	3.561173	-0.54155
15	H	0.19547	-0.73876	4.492045	0.830481
16	C	-0.1859	0.810524	3.502171	-0.29287
17	H	0.1955	1.011962	4.426933	-0.85298
18	H	0.20804	1.536203	3.457549	0.521003
19	C	-0.35329	2.47386	2.049675	-1.29112
20	H	0.20893	2.618164	1.179743	-1.93164
21	H	0.21643	2.900696	1.828952	-0.31378
22	H	0.17558	2.993172	2.908359	-1.73885
23	C	-0.35389	0.437159	2.508191	-2.48731
24	H	0.21087	0.579346	1.602749	-3.07615
25	H	0.17728	0.910209	3.352252	-3.00848
26	H	0.20551	-0.63366	2.688326	-2.4116
37	C	-0.16807	2.485967	-1.38002	0.632197
38	C	-0.24629	2.045826	-2.05758	-0.51001
39	H	0.21192	1.062925	-1.85249	-0.91857
40	C	-0.19398	2.854177	-3.00542	-1.12691
41	H	0.20385	2.488842	-3.51739	-2.0108
42	C	-0.23052	4.112053	-3.30555	-0.6171
43	C	-0.19661	4.554231	-2.64283	0.523068
44	H	0.20124	5.531655	-2.86603	0.937557
45	C	-0.23026	3.753823	-1.69056	1.139816
46	H	0.20784	4.108375	-1.17737	2.026544
48	H	0.20196	4.737829	-4.04772	-1.09918
49	Mg	1.62359	0.009798	0.671525	0.000492
1	S	-0.6061	-1.53802	-0.11476	-1.49147
27	C	-0.16753	-2.55562	-1.28509	-0.62021
28	C	-0.2456	-2.16437	-1.94401	0.550406

29	H	0.21134	-1.18895	-1.75156	0.982607
30	C	-0.194	-3.01072	-2.85953	1.165287
31	H	0.20365	-2.68198	-3.3576	2.071224
32	C	-0.2305	-4.25986	-3.14483	0.626607
33	C	-0.19665	-4.6541	-2.50011	-0.54124
34	H	0.20115	-5.62407	-2.71177	-0.97869
35	C	-0.22954	-3.81537	-1.58088	-1.1568
36	H	0.20773	-4.13317	-1.08204	-2.06538
47	H	0.20186	-4.91553	-3.86151	1.107477

Table S8. Optimized coordinates (Å) and NPA charges for complex **14**.

Number	Atom	q_{NPA}	x	y	z
1	Zn	0.93478	-0.0098	0.671525	-0.00049
3	S	-0.3869	-1.515	-0.17011	-1.50425
4	N	-0.62458	0.910405	2.392888	-1.13412
5	N	-0.62453	-1.03115	2.320227	1.15218
6	C	-0.33917	2.368621	2.220898	-1.26556
7	H	0.21723	2.803923	2.022836	-0.28705
8	H	0.1766	2.831828	3.115104	-1.70514
9	H	0.20683	2.574708	1.366527	-1.91018
10	C	-0.34079	0.312617	2.546574	-2.47212
11	H	0.20484	-0.76798	2.656044	-2.40157
12	H	0.21229	0.51657	1.654702	-3.06347
13	H	0.17816	0.732543	3.421692	-2.98762
14	C	-0.17417	0.60478	3.554055	-0.27232
15	H	0.20883	1.331809	3.561173	0.541545
16	H	0.19606	0.738758	4.492045	-0.83048
17	C	-0.17442	-0.81052	3.502171	0.292871
18	H	0.19588	-1.01196	4.426933	0.852975
19	H	0.20945	-1.5362	3.457549	-0.521
20	C	-0.33943	-2.47386	2.049675	1.291116
21	H	0.20702	-2.61816	1.179743	1.931639
22	H	0.21764	-2.9007	1.828952	0.31378
23	H	0.17657	-2.99317	2.908359	1.738849
24	C	-0.34055	-0.43716	2.508191	2.487309
25	H	0.21254	-0.57935	1.602749	3.076149
26	H	0.17818	-0.91021	3.352252	3.008479
27	H	0.20408	0.633664	2.688326	2.411598
38	C	-0.1633	-2.48597	-1.38002	-0.6322
39	C	-0.23252	-2.04583	-2.05758	0.510011
40	H	0.21683	-1.06293	-1.85249	0.918566
41	C	-0.19096	-2.85418	-3.00542	1.126905

42	H	0.20351	-2.48884	-3.51739	2.010803
43	C	-0.22758	-4.11205	-3.30555	0.617102
44	C	-0.19463	-4.55423	-2.64283	-0.52307
45	H	0.20158	-5.53166	-2.86603	-0.93756
46	C	-0.22431	-3.75382	-1.69056	-1.13982
47	H	0.20626	-4.10838	-1.17737	-2.02654
49	H	0.20194	-4.73783	-4.04772	1.099183
2	S	-0.38523	1.538022	-0.11476	1.491466
28	C	-0.16308	2.555622	-1.28509	0.620209
29	C	-0.23318	2.164366	-1.94401	-0.55041
30	H	0.21625	1.188954	-1.75156	-0.98261
31	C	-0.19091	3.010723	-2.85953	-1.16529
32	H	0.20335	2.681976	-3.3576	-2.07122
33	C	-0.22785	4.259864	-3.14483	-0.62661
34	C	-0.19448	4.654102	-2.50011	0.54124
35	H	0.20156	5.624074	-2.71177	0.978686
36	C	-0.22386	3.815371	-1.58088	1.156796
37	H	0.20625	4.133165	-1.08204	2.065378
48	H	0.20192	4.91553	-3.86151	-1.10748

Table S9. Optimized coordinates (Å) and NPA charges for complex $[\mathbf{4^H}]^{2-}$.

Number	Atom	q_{NPA}	x	y	z
1	Zn	0.6789	-0.00133	-0.0117	-0.00196
3	S	-0.32344	1.245931	-0.89904	-1.87388
4	S	-0.32456	1.256301	0.872066	1.868235
5	S	-0.3231	-1.24397	1.866629	-0.88625
12	C	-0.15316	2.403809	0.289958	-2.48598
13	C	-0.22121	2.69694	1.512156	-1.83919
14	C	-0.2068	3.631934	2.402139	-2.36926
15	C	-0.27646	4.313614	2.115793	-3.55927
16	C	-0.22409	4.036533	0.907406	-4.21165
17	C	-0.23737	3.101561	0.014428	-3.68669
18	C	-0.15259	2.43498	-0.30478	2.463971
19	C	-0.22235	2.78489	-1.48897	1.775996
20	C	-0.20699	3.733997	-2.37046	2.295254
21	C	-0.27651	4.376574	-2.11091	3.512893
22	C	-0.22398	4.044424	-0.93915	4.205188
23	C	-0.23732	3.093336	-0.05615	3.69248
24	C	-0.15318	-2.39338	2.493132	0.302886
25	C	-0.22095	-2.66577	1.871084	1.542598
26	C	-0.20687	-3.59446	2.412413	2.432456
27	C	-0.27676	-4.29018	3.589922	2.128586

28	C	-0.22402	-4.0342	4.217557	0.902523
29	C	-0.23731	-3.10626	3.680787	0.009334
35	H	0.23131	2.191711	1.755014	-0.90997
36	H	0.18859	3.828723	3.332831	-1.8401
37	H	0.18001	5.040785	2.814961	-3.96698
38	H	0.17936	4.550834	0.657763	-5.13932
39	H	0.19415	2.892781	-0.91844	-4.2045
40	H	0.23172	2.311322	-1.70865	0.824285
41	H	0.18842	3.973994	-3.2725	1.735132
42	H	0.17997	5.115531	-2.80292	3.911563
43	H	0.17938	4.526942	-0.71145	5.155307
44	H	0.19431	2.840122	0.847009	4.242123
45	H	0.23064	-2.14931	0.951882	1.799213
46	H	0.18856	-3.77522	1.902225	3.376887
47	H	0.18002	-5.01244	4.006533	2.827586
48	H	0.17938	-4.56051	5.134495	0.638656
49	H	0.19419	-2.91489	4.1788	-0.93793
2	S	-0.32238	-1.26213	-1.88277	0.888224
6	C	-0.15259	-2.4453	-2.48336	-0.28153
7	C	-0.22219	-2.78195	-1.8144	-1.4806
8	C	-0.20717	-3.73516	-2.33755	-2.35549
9	C	-0.27704	-4.39453	-3.54173	-2.07574
10	C	-0.22408	-4.07537	-4.21575	-0.88978
11	C	-0.23737	-3.1212	-3.69852	-0.01273
30	H	0.23101	-2.29587	-0.87317	-1.71682
31	H	0.18834	-3.96483	-1.7915	-3.26882
32	H	0.17996	-5.13629	-3.94376	-2.76279
33	H	0.17934	-4.57128	-5.15488	-0.64572
34	H	0.19428	-2.8793	-4.23377	0.902062

Table S10. Optimized coordinates (Å) and NPA charges for complex [**16**]$^{2-}$.

Number	Atom	q_{NPA}	x	y	z
1	Cd	1.03517	-0.01563	0.090563	-0.05405
3	S	-0.41464	1.354103	-1.27322	-1.8905
4	S	-0.40521	1.450724	1.336384	1.791503
5	S	-0.40217	-1.28063	2.032746	-1.35729
12	C	-0.1544	2.641319	-0.2893	-2.57194
13	C	-0.22638	3.201712	0.826306	-1.92289
14	C	-0.20518	4.236615	1.549669	-2.49961
15	C	-0.27325	4.761369	1.193112	-3.74019
16	C	-0.22087	4.221657	0.088671	-4.39592
17	C	-0.23679	3.183406	-0.63467	-3.82581

18	C	-0.15792	2.395492	0.206296	2.748952
19	C	-0.22481	2.162624	-1.18082	2.790858
20	C	-0.20533	2.935367	-2.01893	3.583056
21	C	-0.27424	3.96885	-1.51538	4.369981
22	C	-0.2208	4.213706	-0.14385	4.343923
23	C	-0.23623	3.44619	0.696894	3.550626
24	C	-0.15597	-2.51274	2.779614	-0.35218
25	C	-0.22695	-3.08003	2.170418	0.782674
26	C	-0.20586	-4.06902	2.80373	1.522738
27	C	-0.27507	-4.54125	4.064846	1.164622
28	C	-0.22128	-3.99485	4.682474	0.041433
29	C	-0.23705	-3.00211	4.055474	-0.69825
35	H	0.2269	2.824637	1.120591	-0.94993
36	H	0.1895	4.638466	2.406446	-1.96605
37	H	0.18033	5.570243	1.76368	-4.18613
38	H	0.17975	4.609649	-0.21103	-5.36658
39	H	0.19444	2.767081	-1.48858	-4.35
40	H	0.22222	1.359234	-1.60428	2.199652
41	H	0.18946	2.722079	-3.08414	3.583318
42	H	0.1805	4.570587	-2.176	4.986475
43	H	0.17988	5.015577	0.277134	4.945813
44	H	0.1944	3.651049	1.762318	3.535898
45	H	0.22527	-2.74529	1.182942	1.079323
46	H	0.18904	-4.47723	2.298265	2.393505
47	H	0.18008	-5.31456	4.555223	1.747917
48	H	0.17948	-4.34198	5.667876	-0.26046
49	H	0.19444	-2.58024	4.550768	-1.56662
2	S	-0.41191	-1.56779	-1.66175	1.250725
6	C	-0.15719	-2.52383	-2.64845	0.156732
7	C	-0.22391	-2.31325	-2.72048	-1.23266
8	C	-0.2049	-3.0966	-3.53303	-2.04106
9	C	-0.27353	-4.12052	-4.31022	-1.50439
10	C	-0.2205	-4.34474	-4.25342	-0.13026
11	C	-0.2356	-3.56588	-3.44051	0.680624
30	H	0.22131	-1.52006	-2.13599	-1.68368
31	H	0.19003	-2.89887	-3.55679	-3.10891
32	H	0.18083	-4.73041	-4.94303	-2.14163
33	H	0.18022	-5.13878	-4.84703	0.316444
34	H	0.19467	-3.75441	-3.40276	1.748467

Table S11. Optimized coordinates (Å) and NPA charges for complex **7**.

Number	Atom	q_{NPA}	x	y	z
1	Li	0.8267	-1.5978	0.416871	-0.06174
5	N	-0.5695	-2.54217	2.399646	0.024098
6	N	-0.57825	-3.60334	-0.38849	-0.04598
7	C	-0.48027	-1.96785	3.312093	1.023249
8	C	-0.48474	-2.48719	3.018341	-1.30991
9	C	-0.27807	-3.92723	2.048378	0.396897
10	C	-0.27664	-4.4301	0.800174	-0.32732
11	C	-0.48953	-3.86926	-0.9176	1.304165
12	C	-0.48369	-3.86306	-1.43779	-1.04653
13	H	0.22724	-0.94572	3.570548	0.735065
14	H	0.24834	-1.93062	2.817541	1.996746
15	H	0.20468	-2.54444	4.248321	1.114157
16	H	0.23926	-2.86368	2.331145	-2.06932
17	H	0.24033	-1.44904	3.240069	-1.56594
18	H	0.20269	-3.07217	3.953132	-1.35288
19	H	0.22219	-4.6185	2.885866	0.1961
20	H	0.24273	-3.94571	1.878955	1.477386
21	H	0.22349	-5.48544	0.627593	-0.0514
22	H	0.23895	-4.4142	0.968482	-1.40851
23	H	0.2356	-3.60105	-0.1842	2.067075
24	H	0.25276	-3.25207	-1.80199	1.467974
25	H	0.20222	-4.93028	-1.19336	1.429065
26	H	0.23885	-3.61484	-1.06738	-2.04394
27	H	0.20166	-4.91727	-1.76224	-1.03659
28	H	0.25256	-3.22588	-2.29853	-0.83911
30	Li	0.8267	1.597736	0.416863	0.061616
33	N	-0.5695	2.541961	2.399728	-0.02428
34	N	-0.57825	3.603437	-0.38823	0.045945
35	C	-0.48027	1.967479	3.311947	-1.02354
36	C	-0.48473	2.486813	3.018549	1.309667
37	C	-0.27806	3.927086	2.048652	-0.39697
38	C	-0.27664	4.430052	0.800528	0.327321
39	C	-0.48953	3.869415	-0.91721	-1.30424
40	C	-0.48369	3.863336	-1.43754	1.046436
41	H	0.22724	0.945282	3.570211	-0.73544
42	H	0.24833	1.930386	2.817291	-1.99699
43	H	0.20468	2.543861	4.248295	-1.11452
44	H	0.23925	2.863543	2.331551	2.06913
45	H	0.24033	1.448605	3.239982	1.565705
46	H	0.20269	3.071508	3.953524	1.35252

47	H	0.22219	4.61824	2.886226	-0.19612
48	H	0.24273	3.945701	1.87921	-1.47745
49	H	0.22349	5.485426	0.628048	0.051454
50	H	0.23895	4.414071	0.968858	1.408501
51	H	0.23559	3.601041	-0.18381	-2.06709
52	H	0.25276	3.252383	-1.80171	-1.46807
53	H	0.20222	4.930484	-1.19277	-1.42919
54	H	0.23885	3.615087	-1.06723	2.043868
55	H	0.20166	4.917599	-1.76183	1.036459
56	H	0.25256	3.226286	-2.29837	0.838981
2	S	-0.74943	-0.06177	0.21297	1.927564
3	S	-0.01619	0.220547	-1.82317	2.345076
4	S	-0.09394	-0.6395	-3.04516	0.872782
31	S	-0.09395	0.639817	-3.04519	-0.87236
32	S	-0.01619	-0.22036	-1.82355	-2.34486
29	S	-0.74944	0.061597	0.212711	-1.92765

Table S12. Optimized coordinates (Å) and NPA charges for complex **8**.

Number	Atom	q_{NPA}	x	y	z
4	N	-0.67218	2.351538	-0.47041	1.417839
5	C	-0.18545	3.535383	-0.54784	0.53121
6	C	-0.35554	2.514677	0.593203	2.429251
7	C	-0.35265	2.138798	-1.76129	2.103384
8	H	0.19706	4.461906	-0.48465	1.119087
9	H	0.17987	3.371038	0.379447	3.082951
10	H	0.17731	3.012086	-2.03324	2.711339
11	H	0.21431	1.944475	-2.54231	1.369191
12	H	0.20579	3.528814	-1.5303	0.055363
13	H	0.21649	1.611064	0.66028	3.033753
14	H	0.2069	1.269254	-1.68318	2.756601
15	H	0.19928	2.666508	1.560682	1.952288
17	N	-0.67218	2.351542	0.470408	-1.41784
19	C	-0.18545	3.535385	0.547835	-0.5312
21	C	-0.35554	2.514683	-0.5932	-2.42925
22	C	-0.35265	2.138807	1.761294	-2.10338
23	H	0.19706	4.46191	0.484651	-1.11908
24	H	0.20579	3.528816	1.530297	-0.05536
25	H	0.17987	3.371046	-0.37945	-3.08295
26	H	0.21649	1.611072	-0.66028	-3.03375
27	H	0.19928	2.666512	-1.56068	-1.95228
28	H	0.17731	3.012097	2.033233	-2.71133
29	H	0.21431	1.944482	2.542311	-1.36919

30	H	0.2069	1.269264	1.683183	-2.7566
31	Mg	1.61035	0.676053	0.000001	-1E-06
1	S	-0.76498	-0.2712	-2.00615	-0.89933
2	S	-0.03996	-2.01534	-2.17545	0.247104
3	S	-0.03143	-3.43317	-0.89691	-0.54154
16	S	-0.76498	-0.27121	2.006157	0.899327
18	S	-0.03143	-3.43317	0.896906	0.541542
20	S	-0.03996	-2.01534	2.175453	-0.24711

Table S13. Optimized coordinates (Å) and NPA charges for complex **9**.

Number	Atom	q_{NPA}	x	y	z
1	Zn	0.88444	0.608746	0.000007	-8E-06
5	N	-0.62535	2.306555	-0.49554	1.404913
6	C	-0.17512	3.488459	-0.55686	0.521127
7	C	-0.34229	2.461269	0.546191	2.436303
8	C	-0.33835	2.076353	-1.79751	2.05689
9	H	0.1974	4.414913	-0.5026	1.110743
10	H	0.18021	3.308243	0.316412	3.0975
11	H	0.17797	2.940786	-2.08996	2.668674
12	H	0.21366	1.885522	-2.55978	1.3028
13	H	0.20655	3.483413	-1.53048	0.027724
14	H	0.21663	1.550171	0.605405	3.030033
15	H	0.20827	1.198952	-1.72751	2.699919
16	H	0.19907	2.624246	1.521056	1.978932
18	N	-0.62535	2.306576	0.495534	-1.4049
20	C	-0.17512	3.488475	0.556828	-0.5211
22	C	-0.34229	2.461282	-0.54619	-2.4363
23	C	-0.33835	2.076409	1.797515	-2.05687
24	H	0.1974	4.414931	0.502549	-1.11072
25	H	0.20655	3.483447	1.530448	-0.0277
26	H	0.18021	3.30826	-0.31642	-3.09749
27	H	0.21663	1.550186	-0.60539	-3.03003
28	H	0.19908	2.624248	-1.52106	-1.97893
29	H	0.17797	2.940862	2.08996	-2.66863
30	H	0.21366	1.88557	2.559783	-1.30278
31	H	0.20827	1.199025	1.727539	-2.69992
2	S	-0.54535	-0.32241	-1.90038	-0.89105
3	S	0.00328	-2.09596	-2.16807	0.174613
4	S	-0.0188	-3.50914	-0.87048	-0.58375
17	S	-0.54535	-0.32242	1.900384	0.891047
19	S	-0.0188	-3.50914	0.870478	0.583748
21	S	0.00328	-2.09596	2.168071	-0.17462

Table S14. Optimized coordinates (Å) and NPA charges for complex $[\mathbf{6_A}]^{2-}$.

Number	Atom	q_{NPA}	x	y	z
1	Zn	0.67561	0.001305	0.000407	-0.00016
6	S	-0.54259	1.54811	-1.4875	-1.14673
7	S	-0.12602	3.283704	-0.3359	-0.98749
8	S	-0.12605	3.283715	0.33536	0.987478
9	S	-0.54265	1.548533	1.487884	1.146523
2	S	-0.5429	-1.54859	-1.50773	1.122423
3	S	-0.12622	-3.28393	-0.3513	0.982948
4	S	-0.12624	-3.28435	0.350526	-0.98241
5	S	-0.54294	-1.54964	1.507891	-1.12245

Table S15. Optimized coordinates (Å) and NPA charges for complex $[\mathbf{6_B}]^{2-}$.

Number	Atom	q_{NPA}	x	y	z
1	Zn	0.67882	0.001873	-0.00069	0.000139
8	S	-0.48523	1.290838	1.253487	-1.62906
9	S	-0.48519	1.29174	-1.25423	1.628956
10	S	-0.06218	3.016796	1.999517	-0.78751
11	S	-0.06219	3.017939	-1.99912	0.787186
12	S	-0.1221	4.523877	0.566644	-0.8923
13	S	-0.12214	4.524321	-0.56539	0.891773
2	S	-0.48533	-1.29193	1.246672	1.633875
3	S	-0.06214	-3.01604	1.995796	0.791732
4	S	-0.12242	-4.5257	0.565346	0.893063
5	S	-0.12245	-4.52588	-0.5641	-0.89317
6	S	-0.06216	-3.01708	-1.99554	-0.79148
7	S	-0.48528	-1.29239	-1.24779	-1.63334

Table S16. Optimized coordinates (Å) and NPA charges for complex [**10**]$^{2-}$.

Number	Atom	q_{NPA}	x	y	z
1	Cd	1.01047	-0.00219	0.000061	-9.5E-05
8	S	-0.56994	-1.4961	-2.12881	-0.64559
9	S	-0.06486	-3.23786	-1.55061	-1.57959
10	S	-0.11766	-4.67544	-1.04517	-0.16344
11	S	-0.11764	-4.67554	1.044758	0.163314
12	S	-0.06485	-3.238	1.550115	1.57944
13	S	-0.56991	-1.49644	2.128918	0.645512
2	S	-0.57005	1.497074	0.647169	-2.12685
3	S	-0.06475	3.238713	1.580483	-1.5477
4	S	-0.11802	4.677661	0.164901	-1.045
5	S	-0.11801	4.677855	-0.1665	1.044721
6	S	-0.06476	3.237597	-1.58043	1.548142
7	S	-0.57002	1.49705	-0.64501	2.12732

References

1 A. B. Pangborn, M. A. Giardello, R. H. Grubbs, R. K. Rosen, F. J. Timmers, *Organometallics*, 1996, **15**, 1518-1520.

2 R. García-Rodríguez, H. Liu, *J. Phys. Chem. A*, 2014, **118**, 7314-7319.

3 A. Jerschow, N. Müller, *J. Magn. Reson.*, 1997, **125**, 372-375.

4 D. H. Wu, A. D. Chen, C. S. Johnson, *J. Magn. Reson. Ser. A* 1995, **115**, 260-264.

5 R. Evans, G. Dal Poggetto, M. Nilsson, G. A. Morris, *Anal. Chem.*, 2018, **90**, 3987-3994.

6 P.-J. Voorter, A. McKay, J. Dai, O. Paravagna, N. R. Cameron, T. Junkers, *Angew. Chem. Int. Ed.*, 2022, **61**, e202114536.

7 *APEX-3*, Bruker AXS: Madison, Wisconsin, 2016.

8 L. Krause, R. Herbst-Irmer, G. M. Sheldrick, D. Stalke, *J. Appl. Crystallogr.*, 2015, **48**, 3-10.

9 G. Sheldrick, *Acta Crystallogr. A*, 2015, **71**, 3-8.

10 G. Sheldrick, *Acta Crystallogr. C*, 2015, **71**, 3-8.

11 M. J. Frisch, G. W. Trucks, H. B. Schlegel, G. E. Scuseria, M. A. Robb, J. R. Cheeseman, G. Scalmani, V. Barone, G. A. Petersson, H. Nakatsuji, X. Li, M. Caricato, A. V. Marenich, J. Bloino, B. G. Janesko, R. Gomperts, B. Mennucci, H. P. Hratchian, J. V. Ortiz, A. F. Izmaylov, J. L. Sonnenberg, Williams, F. Ding, F. Lipparini, F. Egidi, J. Goings, B. Peng, A. Petrone, T. Henderson, D. Ranasinghe, V. G. Zakrzewski, J. Gao, N. Rega, G. Zheng, W. Liang, M. Hada, M. Ehara, K. Toyota, R. Fukuda, J. Hasegawa, M. Ishida, T. Nakajima, Y. Honda, O. Kitao, H. Nakai, T. Vreven, K. Throssell, J. A. Montgomery Jr., J. E. Peralta, F. Ogliaro, M. J. Bearpark, J. J. Heyd, E. N. Brothers, K. N. Kudin, V. N. Staroverov, T. A. Keith, R. Kobayashi, J. Normand, K. Raghavachari, A. P. Rendell, J. C. Burant, S. S. Iyengar, J. Tomasi, M. Cossi, J. M. Millam, M. Klene, C. Adamo, R. Cammi, J. W. Ochterski, R. L. Martin, K. Morokuma, O. Farkas, J. B. Foresman, D. J. Fox *Gaussian 16 Rev. C.01*, Wallingford, CT, 2016.

12 S. I. Gorelsky, L. Basumallick, J. Vura-Weis, R. Sarangi, K. O. Hodgson, B. Hedman, K. Fujisawa, E. I. Solomon, *Inorg. Chem.*, 2005, **44**, 4947-4960.

13 E. I. Solomon, S. I. Gorelsky, A. Dey, *J. Comput. Chem.*, 2006, **27**, 1415-1428.